

**This is a self-archived version of an original article. This version may differ from the original in pagination and typographic details.**

**Author(s):** Jernfors, Toni; Lavrinienko, Anton; Vareniuk, Igor; Landberg, Rikard; Fristedt, Rikard; Tkachenko, Olena; Taskinen, Sara; Tukalenko, Eugene; Mappes, Tapio; Watts, Phillip C.

**Title:** Association between gut health and gut microbiota in a polluted environment

**Year:** 2024

**Version:** Published version

**Copyright:** © 2024 The Authors. Published by Elsevier B.V.

**Rights:** CC BY 4.0

**Rights url:** <https://creativecommons.org/licenses/by/4.0/>

**Please cite the original version:**

Jernfors, T., Lavrinienko, A., Vareniuk, I., Landberg, R., Fristedt, R., Tkachenko, O., Taskinen, S., Tukalenko, E., Mappes, T., & Watts, P. C. (2024). Association between gut health and gut microbiota in a polluted environment. *Science of the Total Environment*, 914, Article 169804. <https://doi.org/10.1016/j.scitotenv.2023.169804>



# Association between gut health and gut microbiota in a polluted environment

Toni Jernfors<sup>a,\*</sup>, Anton Lavrinienko<sup>a,b</sup>, Igor Vareniuk<sup>c</sup>, Rikard Landberg<sup>d</sup>, Rikard Fristedt<sup>d</sup>, Olena Tkachenko<sup>c</sup>, Sara Taskinen<sup>e</sup>, Eugene Tukalenko<sup>f</sup>, Tapio Mappes<sup>a</sup>, Phillip C. Watts<sup>a</sup>

<sup>a</sup> Department of Biological and Environmental Science, University of Jyväskylä, FI-40014, Finland

<sup>b</sup> Laboratory of Food Systems Biotechnology, Institute of Food, Nutrition and Health, ETH Zürich, Zürich, Switzerland

<sup>c</sup> Department of Cytology, Histology and Reproductive Medicine, Taras Shevchenko National University of Kyiv, 01033, Ukraine

<sup>d</sup> Division of Food and Nutrition Science, Department of Life Sciences, Chalmers University of Technology, SE-412 96 Gothenburg, Sweden

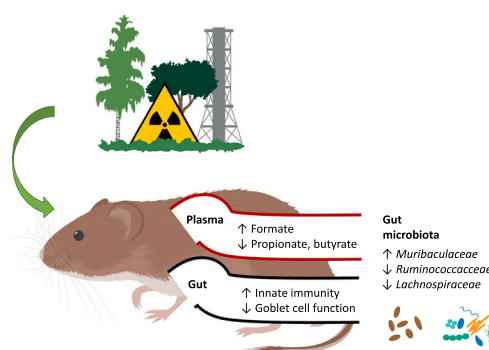
<sup>e</sup> Department of Mathematics and Statistics, University of Jyväskylä, FI-40014, Finland

<sup>f</sup> Department of Radiobiology and Radioecology, Institute for Nuclear Research of NAS of Ukraine, 020000, Ukraine

## HIGHLIGHTS

- We quantified gut health and gut microbiota in wild rodents exposed to radionuclides.
- Exposure to radionuclides was associated with smaller goblet cells and reduced mucus production, and a change in microbiota.
- Exposure to radionuclide contamination was associated with reduced levels of circulating butyrate and propionate.
- Radionuclide exposure impacts host health and physiology, and this likely alters microbiota.

## GRAPHICAL ABSTRACT



## ARTICLE INFO

Editor: Rafael Mateo Soria

### Keywords:

Ecotoxicology  
Habitat degradation  
Radionuclides  
Transcriptomics  
Microbiome  
Histology

## ABSTRACT

Animals host complex bacterial communities in their gastrointestinal tracts, with which they share a mutualistic interaction. The numerous effects these interactions grant to the host include regulation of the immune system, defense against pathogen invasion, digestion of otherwise undigestible foodstuffs, and impacts on host behaviour. Exposure to stressors, such as environmental pollution, parasites, and/or predators, can alter the composition of the gut microbiome, potentially affecting host-microbiome interactions that can be manifest in the host as, for example, metabolic dysfunction or inflammation. However, whether a change in gut microbiota in wild animals associates with a change in host condition is seldom examined. Thus, we quantified whether wild bank voles inhabiting a polluted environment, areas where there are environmental radionuclides, exhibited a change in gut microbiota (using 16S amplicon sequencing) and concomitant change in host health using a combined approach of transcriptomics, histological staining analyses of colon tissue, and quantification of short-chain fatty acids in faeces and blood. Concomitant with a change in gut microbiota in animals inhabiting contaminated areas, we found evidence of poor gut health in the host, such as hypotrophy of goblet cells and likely weakened

\* Corresponding author.

E-mail address: [toni.m.jernfors@jyu.fi](mailto:toni.m.jernfors@jyu.fi) (T. Jernfors).

<https://doi.org/10.1016/j.scitotenv.2023.169804>

Received 27 April 2023; Received in revised form 28 August 2023; Accepted 29 December 2023

Available online 4 January 2024

0048-9697/© 2024 The Authors. Published by Elsevier B.V. This is an open access article under the CC BY license (<http://creativecommons.org/licenses/by/4.0/>).

mucus layer and related changes in *Cla1* and *Agr2* gene expression, but no visible inflammation in colon tissue. Through this case study we show that inhabiting a polluted environment can have wide reaching effects on the gut health of affected animals, and that gut health and other host health parameters should be examined together with gut microbiota in ecotoxicological studies.

## 1. Introduction

Gut microbiota, the community of microbes (principally bacteria) that reside within mammalian gastrointestinal tracts, make important contributions to the health of their hosts (Shreiner et al., 2015) that include digestion of complex and otherwise indigestible foodstuffs to produce useful metabolites (Gentile and Weir, 2018), limiting the ability of pathogens to colonise the gut (Iacob et al., 2019; Pickard et al., 2017), and/or training and regulation of the host's immune system (Hooper et al., 2012). Given the diversity of anthropogenic activities that impact natural environments and wildlife health (Acevedo-Whitehouse and Duffus, 2009; Hauffe and Barelli, 2019), there is much interest in quantifying the associations between the host's experience of a poor-quality environment and the concomitant impacts on gut microbiota and host health. Indeed, variation in habitat quality (Amato et al., 2013) or exposure to various pollutants (Jin et al., 2017) such as heavy metals (Brila et al., 2021; Richardson et al., 2018), radionuclides (Lavrinienko et al., 2018a) and organic compounds such as polycyclic aromatic hydrocarbons (Redfern et al., 2021) and polychlorinated biphenyls (Zhang et al., 2015), for example, associate with a change in composition of gut bacteria. It is typically not known, however, how such changes in gut bacteria community composition affect the delivery of services to the host or associate with aspects of host health.

One of the primary services provided by the gut microbiota is the supply of metabolites to the host (Gentile and Weir, 2018). Key metabolites derived from fermentation by gut bacteria are the short-chain fatty acids (SCFAs), most prominently acetic, propionic, and butyric acids (van der Hee and Wells, 2021). The SCFAs provide nutrition to colonocytes, but also have anti-inflammatory and antioxidative effects as well as regulatory effects on host immune system and energy metabolism (Huang et al., 2017; Kim, 2021), for instance by stimulating fatty acid oxidation (He et al., 2020). The endocrinological effects of SCFAs are mediated by G-protein-coupled receptors in host endocrine and immune cells or by histone deacetylation (van der Hee and Wells, 2021). Disruption to gut microbiota and the supply of SCFAs can have damaging effects on the gut, such as causing inflammatory bowel diseases (Venegas et al., 2019).

A healthy digestive tract helps limit exposure of the host tissues to gut microbiota, antigens and potentially harmful substances. Key to digestive tract barrier function is the mucus layer, a mesh of glycoproteins (mucins) and antibacterial proteins that cover the surface of gut epithelium (Paone and Cani, 2020). The rigid inner mucus layer consists of transmembrane mucins expressed by epithelial enterocytes, and a healthy inner mucus layer is impenetrable to microbes. The outer mucus layer is produced by specialized epithelial cells, goblet cells, that express and secrete mucins and other facilitating components by exocytosis (Birchenough et al., 2015). Crucially, the porous outer mucus layer is inhabited by mutualist microbes, where they derive nutrients and interact with the host's immune system (Schroeder, 2019). Not only do properties of the gut mucus layer affect the gut microbiota composition, but the gut microbiota can affect the development and composition of the mucus layer (Birchenough et al., 2015; Hooper et al., 1999; Schroeder, 2019). Indeed, gut mucus layer defects are often observed in diseases such as metabolic syndrome-related dysglycemia (Chassaing et al., 2017) and colitis in humans and mice (Johansson et al., 2014). However, impacts of exposure to pollution on gut microbiota and gut health remains understudied in wildlife.

The mammalian gut microbiota harbours hundreds or thousands of taxa, making it functionally diverse (Tian et al., 2020). However, a

change in microbiota community composition does not necessarily elicit a change in function because different taxa may provide similar services (Moya and Ferrer, 2016), a concept known as functional redundancy (Tian et al., 2020). For example, members of the Firmicutes and nine other bacterial phyla have genes associated with production of the short chain fatty acid butyrate (Vital et al., 2014). Indeed, it has proven hard to reconcile inter-individual variation in gut bacteria community composition with variation in metabolite profiles (Rojo et al., 2015). One implication of functional redundancy in microbiota is that a significant change in microbiota composition may have little functional relevance for host health (Moya and Ferrer, 2016). Understanding the interplay between the host, its experience of the environment, and the gut microbiota is important given the current extent of anthropogenic impacts on natural environments that impact wildlife health (Acevedo-Whitehouse and Duffus, 2009; Hauffe and Barelli, 2019).

A well-studied example of a polluted environment is the region surrounding the former Chernobyl nuclear power plant in Ukraine. On April 26, 1986, an accident at reactor 4 of the power plant resulted in the release of about 9 million terabecquerels of radionuclides into the atmosphere, with fallout largely affecting Eastern Europe, Western Russia and Fenno-Scandinavia (Mousseau, 2021). To limit human exposure to high concentrations of environmental radionuclides, the Chernobyl Exclusion Zone (CEZ) was established at an approximately 30 km radius around the accident site (Mousseau, 2021). Wildlife inhabiting the CEZ provide the best-studied models of possible biological impacts of exposure to environmental radionuclides (Lourenço et al., 2016; Mousseau, 2021). Today, the biologically most relevant radioisotopes in the area are cesium-137 whose water-soluble salts easily spread through the ecosystem, and strontium-90, which deposits in bones as a calcium analogue (Beresford et al., 2020). While both radioisotopes have low toxicity, exposure to them is a concern as they are beta-emitters, and high dose of radiation can cause DNA damage and oxidative stress (Desouky et al., 2015; Einor et al., 2016). Effects from radionuclide exposure have been found on multiple biological levels (Lourenço et al., 2016; Mousseau, 2021). For example within populations radionuclide exposure is linked to a decline in abundance in many species, including mammals (Kesäniemi et al., 2019a), soil invertebrates (Møller and Mousseau, 2018), and birds (Garnier-Laplace et al., 2015). Studies in large mammals have found few effects of radionuclide exposure on abundance (Deryabina et al., 2015). Other studies have indicated an increase in mutation rates associated with radionuclide exposure (Car et al., 2022; Møller and Mousseau, 2015). Within individuals, radionuclide exposure has been linked with diverse health problems, including increase in tumours and albinism (Møller et al., 2013), increased parasite load (Morley, 2012) and size reduction in the brain and other organs (Kivisaari et al., 2020; Møller et al., 2011). Somewhat surprisingly, whether radionuclide exposure impacts gut health of wild animals is poorly understood, despite the gastrointestinal tract being the first routes of impact by ingested radionuclides.

The bank vole (*Myodes glareolus*), a small rodent that inhabits mixed woodlands of much of northern Europe and Asia (Macdonald, 2006), was among the first mammals to recolonize contaminated areas within the CEZ following the accident (Baker et al., 1996), and consistently carries some of the highest radionuclide loads among local wildlife (Beresford et al., 2020; Chessier et al., 2000) likely due to its opportunistic diet of forest floor food items. The radiation doses experienced by the bank voles are apparently insufficient to cause detectable DNA damage (Rodgers et al., 2001; Rodgers and Baker, 2000), but there is evidence of elevated diversity in mitochondrial DNA in bank voles

(Baker et al., 2017) inhabiting the CEZ. Some form of adaptation or acclimation to radionuclide exposure appears to have taken place, as skin fibroblasts extracted from voles native to contaminated areas of the CEZ are resistant to treatment by reactive oxygen radicals and other genotoxic agents (Mustonen et al., 2018). Regardless, exposure to radionuclides associates with poor health. For example, bank vole populations in contaminated areas within the CEZ exhibit an increase in frequency of cataracts (Lehmann et al., 2016) and a reduction in population densities and litter sizes (Mappes et al., 2019); moreover, bank voles exposed to radionuclides show signs of metabolic remodelling i.e. increase in fatty acid oxidation (Kesäniemi et al., 2019a), telomere and mitochondrial damage (Kesäniemi et al., 2020, 2019b), and changes in genome architecture (Jernfors et al., 2021).

Some impact of radionuclide exposure on gut health is possible because the gut microbiota of bank voles inhabiting areas contaminated by radionuclides differ to the gut microbiota of animals from uncontaminated areas (Lavrinenko et al., 2018a, 2020), with comparable effects in other rodents (*Apodemus* mice) inhabiting the CEZ and at the Fukushima nuclear accident site in Japan (Lavrinenko et al., 2021). Radionuclide exposure appears to mostly drive changes in member taxa of families *Ruminococcaceae*, *Lachnospiraceae* and *Muribaculaceae* (previously S24–7), although it is not possible to use a general Firmicutes: Bacteroidetes ratio as an indicator of radionuclide exposure because the gut microbiota changes with season (Lavrinenko et al., 2021). Considering the increase in fatty acid oxidation (Kesäniemi et al., 2019a), a change in gut microbiota associated with exposure to radionuclides (Lavrinenko et al., 2018a) and the likelihood that ingestion of radionuclides first impact the gut, we considered two scenarios: 1) a change in gut microbiota leads to a detectable change in services (e.g. SCFAs) provided to host and a concomitant change in host metabolism and/or gut health, or 2) radionuclides impact the host which may affect the gut microbiota, but there is little impact on delivery of services (possibly due to functional redundancy). As key features of gut health we conducted histological examination and RNA sequencing of colon tissue and quantified the gut microbiota using 16S amplicon sequencing. Also, we quantified SCFAs in blood and faecal matter. We found that changes in host physiology and gut microbiota are associated with radionuclide contamination, but the few impacts on faecal SCFAs associated with radionuclide exposure imply that a change in gut microbiota does not necessarily elicit a major change in services they provide to the host.

## 2. Materials & methods

### 2.1. Sample collection

Forty-five female bank voles were live-captured (using Ugglan Special2 live traps) from mixed forest habitats in October 2017 from four general study areas in Ukraine: the (1) east and (2) west side of Dnipro river near Kyiv, and from (3) Gluboke lake and (4) Vesnyane within the CEZ (Fig. S1), henceforth referred as uncontaminated (East and West Kyiv) and contaminated (Vesnyane and Gluboke) groups. At each location 9 or 16 traps were placed in a grid with an inter-trap distance of 15–20 m over one trapping night per trapping site, except at Gluboke lake where two trapping nights were required to obtain sufficient animals. Traps were checked in the following morning and caught animals were transferred to the laboratory for internal absorbed dose rate estimation, body size measurement (body weight and head width), and tissue and faecal sampling.

Faecal samples for microbiota analysis were collected from live animals immediately after capture as in (Lavrinenko et al., 2018a). Next, a sample of whole blood was taken from orbital sinus in heparinized capillary tubes. Animals were then euthanized by cervical dislocation and dissected to collect luminal faecal samples from the colon for SCFA quantification, and tissue samples from mid- and distal colon for histological analyses and RNA sequencing. All faecal samples were immediately stored on dry ice until archived in  $-80^{\circ}\text{C}$  freezer. Colon tissue

samples were stored in Allprotect Tissue Reagent (Qiagen) for RNA extraction and in two different fixatives, 10 % formalin solution and metha-Carnoy solution (60 % methanol, 30 % chloroform, 10 % glacial acetic acid) for histological analyses.

### 2.2. Dosimetry

Ambient radiation levels at each trapping location were measured by averaging at least 9 measurements with a hand-held Geiger counter (Gamma-Scout, GmbH & Co., Germany), placed 1 cm above the ground. Internal absorbed dose rates of bank voles were estimated by measuring  $^{137}\text{Cs}$  activity with SAM 940 radionuclide identifier system (Berkeley Nucleonics Corporation, San Rafael, CA, USA) equipped with a  $3'' \times 3''$  NaI detector (Supplementary Methods 1). A sum of internal and external absorbed dose rates was considered as a total absorbed dose rate per animal (mGy/d), providing means ( $\pm\text{SD}$ ) of  $0.007 \pm 0.002$  mGy/d and  $0.735 \pm 0.504$  mGy/d for uncontaminated and contaminated groups, respectively (Table S1).

### 2.3. Histological analysis of colon tissue

Fixed colon tissue samples were dehydrated, embedded in paraffin, and cut into 5  $\mu\text{m}$  sections. Tissue sections, fixed in 10 % formalin, were stained with hematoxylin and eosin (H&E) for general inspection of tissue condition according to standard protocol (Suvana et al., 2013). Tissue sections fixed in metha-Carnoy solution were stained with alcian blue (Suvana et al., 2013), but counterstained with carmine for visualization of goblet cells. To remove potential bias, histological examination of the colon tissue was performed (by IV and OT) without knowledge of the samples' origins (i.e. a "blind" analysis). Digital microphotographs of stained colon sections were taken at  $\times 100$  or  $\times 400$  magnification using a computer-assisted image analyzing system consisting of Olympus BX41 microscope and Olympus C-5050 Zoom digital camera. Depth of crypts ( $\mu\text{m}$ ), height of colonocytes ( $\mu\text{m}$ ), area of colonocytes' nucleus ( $\mu\text{m}^2$ ) from H&E images, and the cellular area of goblet cells ( $\mu\text{m}^2$ ) from alcian blue–carmine images were measured using Image J v.1.42q (Schneider et al., 2012). Animals were defined as having normal, hypertrophic or hypotrophic goblet cells based on cell size and prevalence of mucus-containing vesicles.

### 2.4. SCFA quantification in blood plasma and faecal samples

SCFAs (formic, acetic, propionic, isobutyric, butyric, succinic, isovaleric, valeric and caproic acids) in plasma were analyzed by liquid chromatography–mass spectrometry (LC–MS) according to method described by (Han et al., 2015), with modifications described in Iversen et al. (2022) (Supplementary Methods 2). Samples were analyzed using a 6500+ QTRAP triple-quadrupole mass spectrometer (AB Sciex, 11432 Stockholm, Sweden), which was equipped with an APCI source and operated in the negative-ion mode. Chromatographic separations were performed on a Phenomenex Kinetix Core-Shell C18 (2.1, 100 mm, 1.7  $\mu\text{m}$  100 Å) UPLC column with SecurityGuard ULTRA Cartridges (C18 2.1 mm ID). SCFAs (acetic, propionic, isobutyric, butyric, isovaleric, valeric and caproic acids) in faecal samples were analyzed by gas chromatography–mass spectrometry (GC–MS) using a Shimadzu GC–MS–TQ8030 (Tokyo, Japan), fast scanning triple quadrupole gas chromatography system with a PAL autosampler (Cheng et al., 2020) (Supplementary Methods 2).

### 2.5. RNA sequencing of colon tissue and de novo assembly

Total RNA was extracted from colonic tissue samples using an RNeasy Mini Kit (Qiagen) according to manufacturer's protocol. Samples were sent to the Beijing Institute of Genomics (BGI), Hong Kong ([www.bgi.com/global/](http://www.bgi.com/global/)) for library preparation and sequencing. RNA libraries were prepared using TruSeq Stranded mRNA Library Prep Kit



(Illumina) and sequenced for 100 bp paired end (PE) reads on two lanes on Illumina HiSeq4000 resulting in depth of ~16 million PE reads per sample (Table S2). Adapters and low quality bases (QS < 20) were removed using SOAPnuke (Chen et al., 2018).

Reads from eight samples (two samples from each study area, providing a total of 143,691,087 PE reads) were pooled for de novo transcriptome assembly using Trinity v.2.5.1 (parameters: default) (Grabherr et al., 2011), followed by transcript clustering using cd-hit-est v.4.6.8 (parameters: -c 0.98 -p 1 -d 0 -b 3) (Fu et al., 2012). Transcriptome completeness was estimated by the presence of assembled single copy orthologs using BUSCO v.2.0 with mammalian lineage dataset odb9 as a reference (Simão et al., 2015). Transcriptome was annotated using the Trinotate v.3.0.1 pipeline (Bryant et al., 2017), leveraging SwissProt 2018\_2 for transcript identification. Downstream analyses followed Trinity best-practice guidelines (Haas et al., 2013) using default parameters, with Bowtie v.1.2.2 (Langmead et al., 2009) used to align reads against the transcriptome and RSEM v.1.3.1 (Li and Dewey, 2011) for alignment counting (transcripts and genes). The colon transcriptome assembly (after clustering with cd-hit-est) consisted of 356,050 transcripts (237,648 genes) that had a contig N50 = 2109 and an E90N50 = 3145 (Table S3). The assembly contained 86 % complete mammalian BUSCOs, and 105,799 transcripts received at least one GO-term annotation.

## 2.6. Gut microbiome amplicon sequencing and bioinformatics analyses

Total DNA was extracted from faecal samples ( $n = 45$ ) using a PowerFaecal DNA Isolation Kit (Qiagen) following the manufacturer's instructions. All library preparation and sequencing work was performed at the BGI. Briefly, samples were processed using the Earth Microbiome Project protocol to amplify the V4 region of the 16S ribosomal RNA (rRNA) gene using the original 515F/806R primers (Caporaso et al., 2011). Libraries were sequenced on an Illumina HiSeq 2500 platform at BGI to provide 250 bp paired-end (PE) reads.

Read data were de-multiplexed, and adapters and primers were removed by BGI. The PE reads (total = 9,790,549, mean = 217,567, range = 129,304–268,333) were processed using QIIME2 v.2018.8 (Bolyen et al., 2019). Briefly, reads were truncated at the 3' end to remove low-quality bases (reverse reads at 186 bp), after which data were denoised using default parameters in dada2 (Callahan et al., 2016). The resulting feature-table contained 5,208,639 sequences, with 3453 sequence variants (SVs). Low-abundance (frequency < 10 across all samples) SVs were removed to leave 5,207,788 reads (mean = 115,728, range = 74,172–137,640 reads per sample) and 3310 SVs. We assigned taxonomy using a naïve Bayes classifier that had been pretrained on the Greengenes v.13.8 16S rRNA gene sequences (reads trimmed to the V4 region amplified by 515F/806R primers, and clustered at 99 % identity) (Bokulich et al., 2018). The final feature-table was rarefied to 74,172 reads per sample.

## 2.7. Statistical analyses

Statistical testing was conducted using R v.4.0.2 (The R Core Team, 2018), using Pearson correlation to test for correlation between logarithm of internal dose rate and various parameters, or Wilcoxon rank sum tests or Kruskal-Wallis tests when comparing medians of various parameters among contaminated and uncontaminated groups or among all four study areas, respectively.

### 2.7.1. Bank vole health and gene expression

Body condition index (BCI) reflecting general physiological condition of the voles was calculated as standardized residuals from linear regression of weight and head width (Labocha et al., 2014). Also, normalized liver and spleen weights were calculated as standardized residuals from a linear regression of organ weight and head width. Exploratory data analysis of host variables (logarithm of internal

absorbed dose rate, morphometric and histological measurements of the colon and SCFA concentration in blood) was conducted using by principal component analysis (PCA) using the package 'FactoMineR' v.1.34 (Lê et al., 2008). An odds ratio for risk of incidence of colon goblet cell hypotrophy or abnormality (either hypo- or hypertrophic) classification in colonic goblet cells in contaminated versus uncontaminated groups was calculated using package 'fmsb' v.0.7.1 (Nakazawa, 2019). A pseudocount was added to odds ratio calculation for hypotrophy incidence due to zero occurrence of hypotrophic goblet cells in uncontaminated group.

A principal component analysis of transcript counts was performed within the Trinity pipeline to summarise the main differences in transcript (gene) expression among samples. Differential expression (DE) analysis between uncontaminated and contaminated groups and between categories of goblet cell (normal, hypotrophic, and hypertrophic) was conducted using DESeq2 in Bioconductor v.3.7 (Love et al., 2014) with DE threshold fold change >2 and a false discovery rate (Benjamini-Hochberg's *FDR*) of <0.05. Gene ontology (GO) term enrichment analysis among differentially expressed transcripts and genes was performed using Goseq in Bioconductor v.3.7 (Young et al., 2010) to identify significantly enriched GO terms (*FDR* < 0.05) using the assembled transcriptome as reference database. We specifically tested difference in expression of five goblet cell secreted mucosal genes, *Muc2*, *Clca1*, *Fcgbp*, *Agr2* and *Zg16* (Birchenough et al., 2015; Paone and Cani, 2020), between the three goblet cell types (normal, hyper- and hypotrophic) using a Kruskal-Wallis test.

### 2.7.2. Gut microbiota composition

Alpha diversity was characterised as species richness (number of SVs) and evenness (Shannon index). Linear discriminant analysis Effect Size (LEfSe) (Segata et al., 2011) was calculated using Galaxy web interface (<https://galaxyproject.org/learn/visualization/custom/lefse/>) to determine the microbial families that explain compositional differences between contaminated and uncontaminated groups, using LDA score thresholds of >2 and <-2,  $p < 0.05$ . ALDEx2 v.1.11.0 (Fernandes et al., 2014) was used to identify differentially abundant SVs (*FDR* < 0.05) between contaminated and uncontaminated groups, and between goblet cell types.

PERMANOVA with Jaccard, Bray-Curtis and unweighted and weighted UniFrac distance metrics that represent compositional differences between samples ( $\beta$ -diversity) was used to simultaneously test the response of the gut microbiota to internal dose, colon goblet cell status and variation in gene expression as principal component scores on components 1 and 2 of transcript count PCA data (Anderson, 2017). PERMANOVA was carried out using the *adonis* function (999 permutations) in *vegan* v.2.5-6 (Oksanen et al., 2018).

## 3. Results

### 3.1. Effects of radionuclide contamination on bank vole health and gene expression

We first performed principal component analysis, incorporating logarithm of internal absorbed dose rate, body condition index, cross-sectional areas of colonic enterocytes and goblet cells, and concentrations of SCFAs in blood to examine general patterns in bank vole physiological characteristics. Clustering of samples appeared to be mainly driven by internal dose rate, goblet cell size and blood propionate and formate concentrations (Fig. 1) along the first two axes (combined eigenvalue 46.9 %). Of the circulating SCFAs in blood, concentration of propionate ( $R = -0.53$ ,  $p < 0.001$ ) and butyrate ( $R = -0.31$ ,  $p < 0.05$ ) had a significant negative correlation with internal dose rate, and formate ( $R = 0.54$ ,  $p < 0.001$ ) having a positive correlation (Fig. S2). Interestingly, formate concentration in bank vole plasma (>300  $\mu\text{M}$ ) was about threefold greater than that reported for laboratory rodents and humans (10–100  $\mu\text{M}$ , Table S4) (Brosnan and Brosnan, 2016;

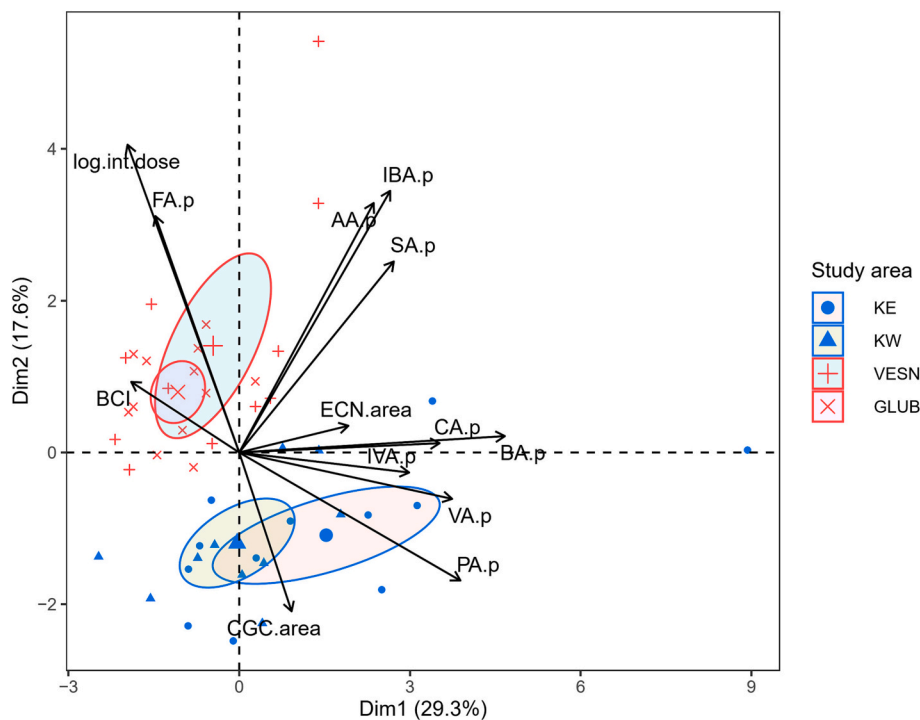


**Fig. 1.** Principal component analysis of host phenotypic variables. Data incorporates logarithm of internal absorbed dose rate, body condition index, cross-sectional areas of colonic enterocytes and goblet cells, and concentrations of SCFAs in blood.

Pietzke et al., 2019). Goblet cell size was negatively correlated with internal dose rate ( $R = -0.37$ ,  $p < 0.05$ ) (Fig. 2D), suggesting an effect on colon health. Bank vole body condition index was not correlated with internal dose rate, consistent with earlier studies (Kesäniemi et al., 2019a).

PCA of transcript counts showed that samples from contaminated and uncontaminated areas were separated on the first two principal components (combined eigenvalue 10.25 %), predominantly on the second principal component PC2 (Fig. 2F), with sample scores along PC2 having a significant, negative correlation with internal dose rate ( $R = -0.62$ ,  $p < 0.001$ ), indicating a general difference in transcriptional activity of the colon between contaminated and uncontaminated groups of samples. Using DESeq2 we identified 98 transcripts (66 genes) that were significantly differentially expressed (DE) (fold change  $> 2$ , FDR  $< 0.05$ ) between samples from contaminated and uncontaminated areas (Table S5), with 68 (and 43) being up-regulated in samples from contaminated areas. DE genes appear to mostly represent activation and/or signaling in the innate immune system, with significant upregulation most prominently in interferon-inducible GTPase I and Schlafen family (SLFN) members 12 and 13 (Table S5). There were too few annotated DEGs to identify significantly enriched gene ontology (GO) terms, however on the transcript level, GO terms associated with innate immunity were detected among upregulated transcripts, including e.g., GO:0002429 'immune response-activating cell surface receptor signaling pathway', GO:0038096 'Fc-gamma receptor signaling pathway involved in phagocytosis', GO:0030449 'regulation of complement activation' and GO:0002673 'regulation of acute inflammatory response' (Table S6).

Histological examination of colon tissue using H&E staining revealed no obvious gross pathological changes such as edema, leukocyte infiltration, disturbance in crypt structure, or superficial epithelium in bank voles inhabiting contaminated (or uncontaminated) areas (pers. obs. by IV). However, alcian blue–carmine staining showed that eight out of 23 animals from contaminated areas (three from Vesnyane and five from Gluboke) exhibited hypotrophic goblet cells, characterised by a reduction in the amount of stained mucin bodies and a low cross-sectional

area (Fig. 2C) which indicates an impaired mucus-producing capability by these cells. Hypotrophic goblet cells were not observed in the animals inhabiting uncontaminated areas. Six animals in total also exhibited goblet cell hypertrophy, although this was not radionuclide related as they occurred equally among contaminated and uncontaminated groups (Fig. 2B). The odds of animals inhabiting contaminated areas exhibiting hypotrophy was 13 times higher than uncontaminated animals (95 % confidence interval = 1.5–112.4, adding pseudocount) (Fig. 2E). To determine whether goblet cell state was accompanied with associated changes in expression of secreted mucosal genes to the outer mucus layer, we specifically tested difference in *Muc2*, *Clca1*, *Fcgbp*, *Agr2* and *Zg16* (Birchenough et al., 2015; Paone and Cani, 2020) mean expression between animals classified with having normal, hypo- and hypertrophic cells. *Clca1* showed significant downregulation in hypotrophic cells compared to hypertrophic cells (Kruskal-Wallis  $H = 11.02$ ,  $df = 2$ ,  $p < 0.01$ , post-hoc Wilcoxon  $p < 0.05$ ) but not compared with normal cells (Fig. 2H). *Agr2* showed downregulation in both hyper- and hypotrophic cells compared to normal cells (Kruskal-Wallis  $H = 6.52$ ,  $df = 2$ ,  $p < 0.05$ ), although post-hoc comparisons showed a weak effect ( $p < 0.1$ ) (Fig. 2G). *Agr2* also negatively correlated with internal dose rate ( $R = -0.36$ ,  $p < 0.05$ ).

### 3.2. Effect of radionuclide contamination on bank vole gut microbiota and faecal SCFAs

We identified 3310 SVs from 12 bacterial phyla in the bank vole gut microbiota (Fig. S3, S4). Three bacterial phyla accounted for 96 % of the gut microbiota community: Firmicutes (mean = 46 %), Bacteroidetes (44 %), and Proteobacteria (6 %). Bacteroidetes were dominated by members of the *S24-7* (*Muribaculaceae*) family (93 % of Bacteroidetes, 42 % of total community), while Firmicutes mainly comprised three families: *Ruminococcaceae* (40 %), *Lachnospiraceae* (25 %), an unidentified family of order Clostridiales (21 %) and *Lactobacillaceae* (3.2 %). This community composition is typical for the gut microbiota of bank voles (Brila et al., 2021) and other wild rodents (Lavrinienko et al., 2021; Maurice et al., 2015).

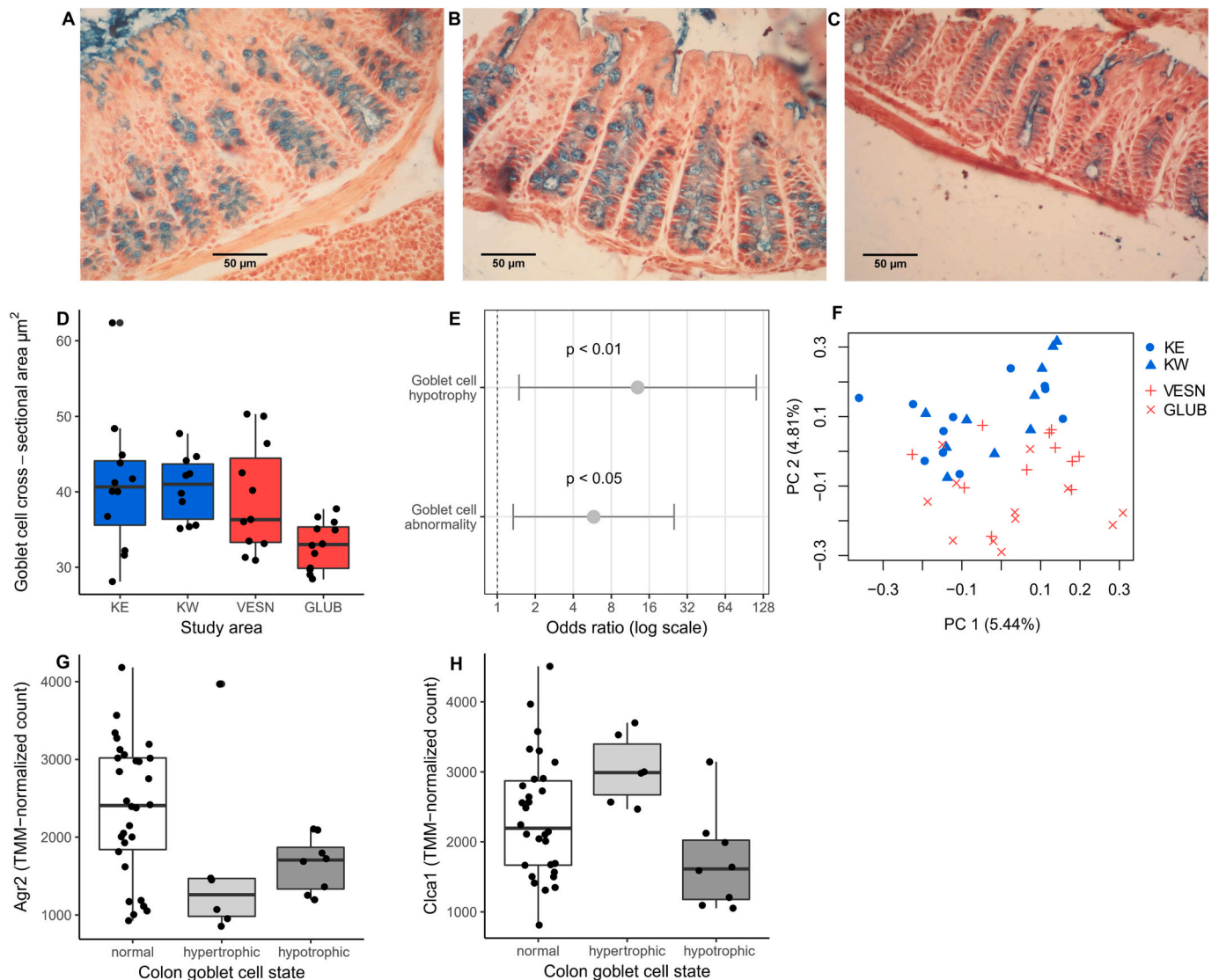


**Fig. 2.** Analyses of bank vole colon tissue health. A) Histological imaging of normal, B) hyper- and C) hypotrophic colonic mucous goblet cells (alcian blue with carmine supplementation;  $\times 400$ ). Mucin bodies (in blue) appear smaller and fewer in number in hypotrophic goblet cells than normal. D) Goblet cell cross-sectional area across study areas. E) Odds ratio of bank voles exposed to radionuclides exhibiting goblet cell hypotrophy and abnormality (hyper+hypotrophic cells). F) Principal component analysis of transcript data. The scores exhibit clustering between treatment groups along component 2. G) Expression levels of *Agr2* and H) *Clca1* across goblet cell health states.

LEfSe analysis of bacterial phyla showed significant increase in Bacteroidetes relative to Firmicutes, Tenericutes and Actinobacteria in contaminated areas compared to uncontaminated areas (Fig. 3C, S3–4), with 21.7 % increase in proportion of Bacteroidetes and a 17.7 % decrease in Firmicutes. In further detail, LEfSe analysis revealed fifteen bacterial families that exhibited a significant difference in proportion between samples from contaminated and uncontaminated groups (LDA-score  $> 2$  or  $< -2$ ,  $p < 0.05$ ) (Fig. 3D). Most prominently, *Muribaculaceae* (Bacteroidetes) were increased in proportion in animals from the CEZ, while decrease in Firmicutes was attributed to five families of Clostridiales: *Ruminococcaceae*, *Lachnospiraceae*, *Syntrophomonadaceae*, *Clostridiaceae* and *Mogibacteriaceae*. At the SV level, ALDEx2 analysis identified 17 SVs whose abundance significantly differed between contaminated and uncontaminated groups ( $FDR < 0.05$ ) (Table 2, Fig. S5), including four members of *Muribaculaceae* with a positive association with the CEZ and ten members of Clostridiales with both positive and negative associations. Notably, *Lactobacillus salivarius*, a probiont (Chaves et al., 2017), showed a strong decrease in the colon of bank voles in the CEZ.

Within-sample species richness was negatively correlated with internal dose rate ( $R = -0.35$ ,  $p < 0.05$ ) (Fig. 3A). There was no significant correlation between internal dose and evenness (Shannon index) however (Fig. 3B), indicating that radionuclide exposure has mostly affected species membership over composition in general. PERMANOVA (999 permutations) model incorporating internal dose rate, goblet cell health state and general patterns of gene expression (sample scores on first two principal components of transcript count PCA) showed that internal dose rate, but not goblet cell state, was a strong predictor of between-sample differences in bank vole gut microbiota community composition (beta diversity) using all four distance metrics (Jaccard, Bray-Curtis, unweighted and weighted UniFrac, Table 1A, Fig. 4). Gene expression patterns were also significant predictors to a lesser degree. Further, we ran an alternative model where gene expression PC scores and goblet cell state were replaced with expression levels of mucosal genes *Clca1* and *Agr2* that previously showed significant variation among goblet cell health states. Here, *Clca1* expression significantly explained variation using Jaccard and Bray-Curtis metrics, but not with UniFrac metrics, likely due to the fact that only few specific SVs are

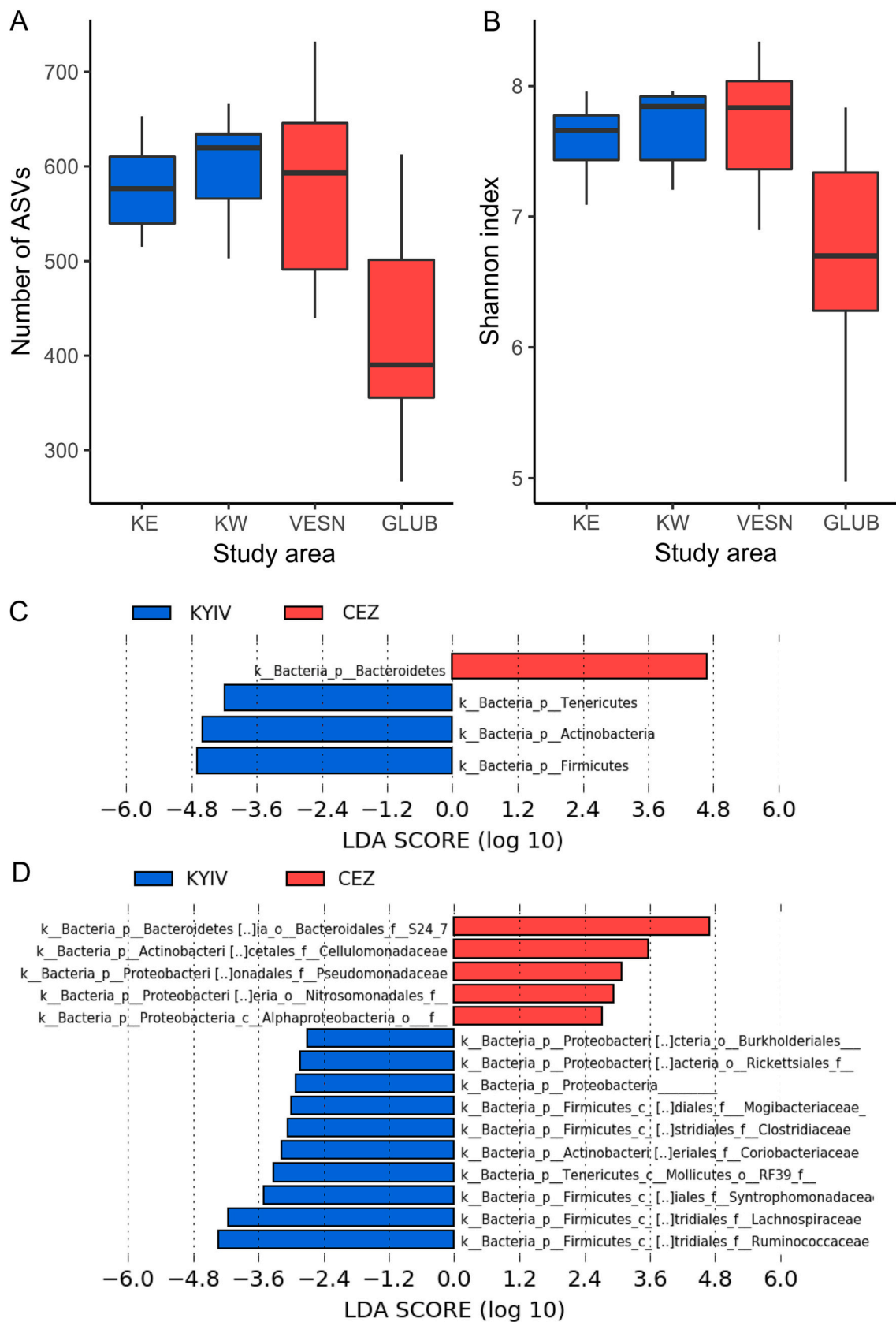


**Fig. 3.** Community composition analyses of bank vole colonic microbiota. A-B: alpha diversity statistics across study areas. Species richness is measured as number of A) unique ASVs and B) evenness as Shannon index. C-D: LEfSe analysis of gut microbiota composition showing differentially abundant taxa between CEZ and Kyiv. Log-transformed LDA-scores for different C) bacterial phyla D) families are shown.



**Table 1**  
PERMANOVA results (999 permutations) of various variables performed on gut microbiome composition using four distance metrics. Modelled as: A) *log internal dose rate* + *goblet cell health state* + *Gene expression PC1* + *Gene expression PC2*. B) *log internal dose rate* + *Clca1* + *Agr2*. Goblet cell health state: three-factor classification of colonic goblet cells into normal, hypo- and hypertrophic cells. Gene expression PC: principal components of gene expression data.

Variable	Jaccard			Bray-Curtis			Unweighted UniFrac			Weighted UniFrac		
	R2	F		R2	F		R2	F		R2	F	
A)												
Log internal dose rate	0.072	3.33	***	0.064	2.96	***	0.058	2.58	***	0.058	3.09	*
Goblet cell health state	0.044	1.01		0.044	1.02		0.047	1.05		0.042	1.11	
Gene expression PC1	0.032	1.48	**	0.033	1.54	*	0.023	1.03		0.115	6.17	**
Gene expression PC2	0.030	1.37	*	0.036	1.67	**	0.026	1.18		0.073	3.92	**
B)												
Log internal dose rate	0.072	3.30	***	0.064	2.93	***	0.058	2.58	***	0.058	2.69	*
Clca1	0.029	1.34	*	0.037	1.70	**	0.026	1.19		0.040	1.88	
Agr2	0.023	1.07		0.025	1.15		0.024	1.07		0.041	1.90	

\*\*\*  $p < 0.001$ .  
\*\*  $p < 0.01$ .  
\*  $p < 0.05$ .

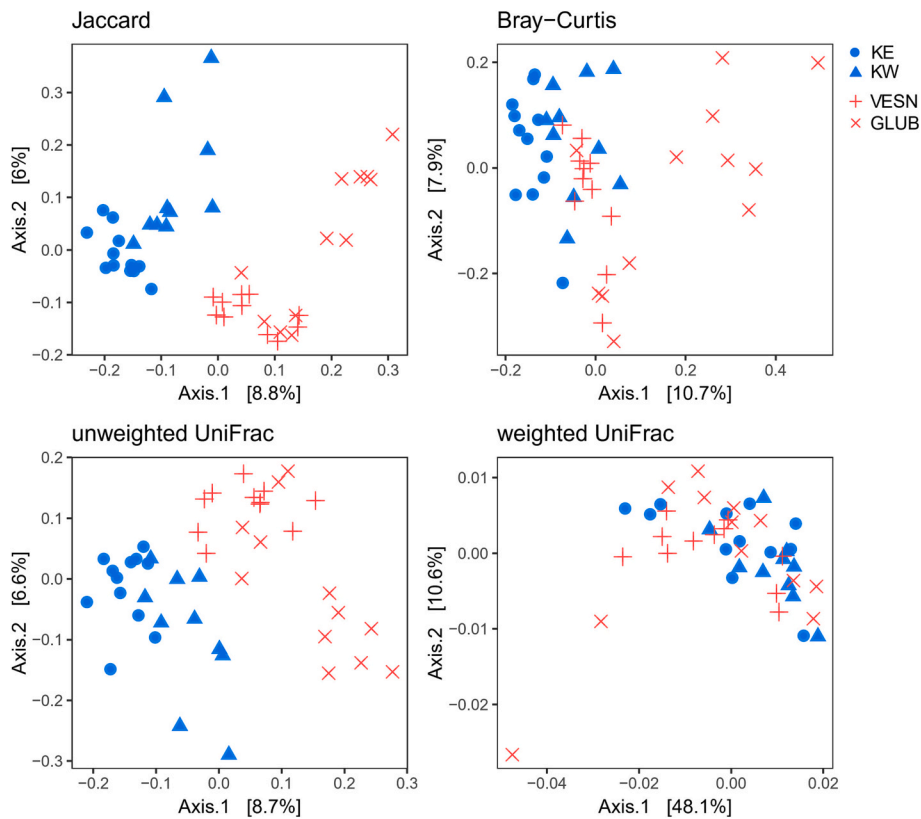


**Fig. 4.** PCoA of radiation-associated differences in bank vole gut microbiota community composition using Bray-Curtis, Jaccard, and unweighted and weighted UniFrac distance metrics.

responsible for majority of compositional changes (Table 2). *Clca1* expression level thus affects abundance of specific SVs.

Although internal dose was a strong predictor of community composition changes using all beta-diversity metrics, these changes were not reflected in SCFA concentrations in faeces. The major SCFAs, acetate, butyrate and propionate were not significantly correlated with logarithm of internal dose rate, but two minor SCFAs, valerate ( $R = -0.35$ ,  $p < 0.05$ ) and caproate ( $R = -0.59$ ,  $p < 0.001$ ) were negatively correlated with logarithm of internal dose rate.

4. Discussion

While changes in gut microbiota can be readily associated with variation in the host’s habitat, including exposure to pollution, it is rarely known whether any difference in the gut microbiota associate with some alteration to health of the host and/or possible services provided by the microbiota. Here, we quantified the associations between host health gut microbiota and variation in one of the key services (faecal SCFAs) provided by the gut microbiota in wild bank voles exposed to environmental radionuclides. We show that (1) exposure to radionuclides is associated with a change in gut microbiota composition, and, crucially, that changes in gut microbiota associate with altered gut

**Table 2**

Differentially abundant ASVs ( $FDR < 0.05$ ) between contaminated and uncontaminated groups. Positive effect size indicates increased relative abundance in animals from the CEZ. Overlap indicates proportion of effect size that overlaps 0 (no effect).

Phylum/order	ASV	Effect size	Overlap	p-Value	FDR
Bacteroidales/Bacteroidales	S24-7 family member 1	1.629853	0.06108	1.04E-07	6.84E-05
	S24-7 family member 2	0.967744	0.193754	0.002319	0.038966
	S24-7 family member 3	0.779687	0.178267	0.000155	0.024177
	S24-7 family member 4	0.672805	0.135653	0.000357	0.037049
Firmicutes/Lactobacillales	<i>Lactobacillus salivarius</i>	-1.51825	0.083038	9.40E-07	0.000301
Firmicutes/Clostridiales	Clostridiales order member 1	-0.89611	0.198013	0.000185	0.02148
	Clostridiales order member 2	-0.91012	0.198723	0.000615	0.034021
	Clostridiales order member 3	-1.11462	0.088715	3.82E-05	0.003561
	Lachnospiraceae family member	1.123097	0.150568	5.51E-05	0.006997
	Ruminococcaceae family member 1	-1.15595	0.105749	4.56E-05	0.005403
	Ruminococcaceae family member 2	1.470684	0.093684	5.57E-06	0.001387
	Ruminococcaceae family member 3 - genus Oscillospira	1.360572	0.083097	7.97E-07	0.000378
	Ruminococcaceae family member 4 - genus Oscillospira	1.263068	0.086648	2.21E-06	0.000777
	Ruminococcaceae family member 5 - genus Oscillospira	-0.71191	0.154119	0.00061	0.046936
	Ruminococcaceae family member 6 - genus Ruminococcus	0.87122	0.124202	0.000186	0.019826
Spirochaetes/Spirochaetales	Treponema genus member	0.926208	0.192472	0.000555	0.031483
Tenericutes/Mycoplasmatales	Mycoplasmataceae family member	-0.91171	0.171043	0.000299	0.025607

health as (2) bank voles inhabiting contaminated areas exhibit changes in colon morphology (goblet cell morphology) and transcription (immune function, and mucus production). However, it is the (3) levels of circulating SCFAs (formate, propionate, and butyrate) that correlate with absorbed dose rather than the concentrations of faecal SCFAs.

#### 4.1. Effect of environmental radionuclides on the gut microbiota

Exposure to environmental radionuclides associates with compositional changes in gut microbiota in bank voles (Lavrinienko et al., 2020, 2018a, 2018b) and in *Apodemus* mice (Lavrinienko et al., 2021). Interestingly, previous studies found a reduction in Bacteroidetes and an increase in Firmicutes was associated with inhabiting an area contaminated by radionuclides (Lavrinienko et al., 2018b, 2018a), whereas Bacteroidetes increased in proportion in our samples. One explanation for this difference is that wild animal gut microbiota can exhibit marked seasonal changes in composition (Maurice et al., 2015). While there is apparent stability of the gut microbiota community in bank voles inhabiting contaminated areas within the CEZ, bank voles from uncontaminated areas show a reduction in Bacteroidetes and an increase in Firmicutes (principally *Ruminococcaceae* and *Lachnospiraceae*) between May and June (Lavrinienko et al., 2020). By autumn, the bank vole gut microbiota is characterised by enrichment of Bacteroidetes (*Muribaculaceae*) in contaminated areas and an enrichment of Firmicutes (*Ruminococcaceae* and *Lachnospiraceae*) in uncontaminated areas. Similarly, the reduction in alpha diversity in this data that was not observed earlier (Lavrinienko et al., 2018a) may be driven by seasonality. Another complicating factor could be interannual variation in gut composition, which is understudied in terrestrial systems. Nonetheless, a 4-year study of gut microbiota in wild primate *Propithecus verreauxi* communities uncovered weak effects of environmental and seasonal changes compared with properties of the host and social behaviour (Rudolph et al., 2022). In bank voles, an apparent lack of radiation impacts on bank vole gut microbiota sampled during July–August (Antwis et al., 2021) is consistent with seasonal changes in gut microbiota identified using mark-release-recapture studies (Lavrinienko et al., 2020) rather than a lack of effect of radionuclides per se. As gut microbiota of bank voles inhabiting the CEZ is seasonally dynamic, it may be difficult to find a stable biomarker (e.g. enrichment or loss of particular taxa) of exposure. Together with our data, we highlight the need to consider seasonal or interannual variation in gut microbiota together with host ecology/physiology when interpreting possible environmental impacts on wildlife gut microbiota composition (Watts et al., 2022). Nonetheless, the important question remains: does variation in gut microbiota associate with some altered provision of services or host health?

#### 4.2. Impaired gut health in bank voles exposed to radionuclides

The intestinal epithelium is radiosensitive, and indeed, we see an impact on mucus production and immune gene expression. Certainly, an acute dose of radiation (>8 Gy) in clinical settings elicits breakdown of the mucosal layer and activation of the immune system in the human colon (François et al., 2013; Malipatlolla et al., 2019; Moussa et al., 2016), while lower doses (<1 Gy) may attenuate ongoing inflammation (Di Maggio et al., 2015; Frey et al., 2015). Through ingestion of soil particles and radionuclide-accumulating dietary items such as macrofungi (Mousseau, 2021), the bank vole gastrointestinal tract is exposed to chronic doses of radiation. Despite decades of research on impact of radionuclide exposure in wildlife (reviewed by Mousseau, 2021), gut health has consistently been overlooked. Although estimated total absorbed doses in this study varied between 27 and 213 mGy for 2–3-month-old animals, falling within the medium-high total dose rate band defined by the derived consideration reference level (DCRL) for rat reference (ICRP, 2008), the colon tissue of bank voles from contaminated areas did not show obvious signs of pathological damage or inflammation, regardless of apparent antibacterial and/or viral activity in the innate immune system as indicated by upregulation of interferon-inducible GTPase I and SLFN 12 and 13 (Jo and Pommier, 2022). The prevalence of colonic goblet cell hypotrophy however indicates that some animals experience a reduced capacity for mucus production in the colon. This is consistent with reduced transcriptional activity of *Clca1* and *Agr2* in animals exhibiting goblet cell hypotrophy, which are required for correct formation of the outer mucus layer (Nyström et al., 2018; Park et al., 2009), suggesting of radiation stress on colon health. Thus, bank voles inhabiting areas contaminated by environmental radionuclides experience a marked change in the gut environment.

The restricted and uneven distribution of radionuclide contamination within the CEZ makes it challenging to quantify the impacts of radionuclide exposure in wild animals. Studies at one site (i.e. the Red Forest) suffer from lack of replication, such that any apparent effect of radionuclide exposure could be attributed to site-specific habitat. To overcome this challenge, we studied animals from independent contaminated sites, Vesnyane and Gluboke, identify generally consistent impacts of radionuclide exposure that outweigh any effects arising from variation in habitat. Of course, site-specific variation (i.e. in alpha diversity and goblet cell size) is expected in any study of wild animals. For example, Gluboke site has more small rivers that would spatially restrict animal mobility than Vesnyane, which might more easily receive immigrants from less polluted areas. Increasing the number of replicate contaminated areas would involve sampling on a much broader spatial scale (e.g. in Belarus), which would increase the number of habitats. Thus, to further study these biomarkers (e.g. goblet cell size) requires

laboratory experiments.

#### 4.3. Associations between gut microbiota and gut health

Many studies have identified correlates of altered wildlife gut microbiota composition, including exposure to pollutants (Brila et al., 2021), parasites (Cortés et al., 2020) and/or systemic pathogens (Brila et al., 2023), that indicate that a change in gut microbiota associates with a change in host health. Bank voles exposed to radionuclides provide more direct insights into the connections between impacts of pollution on wildlife gut health (described in *Impaired gut health in bank voles exposed to radionuclides* above) and the associated changes in gut microbiota. For instance, reduction of *L. salivarius* in the CEZ could facilitate the increase in potentially pathogenic species such as the unidentified SV of genus *Treponema*, as some species of *Lactobacillus* are probiotics and help prevent colonisation by pathogens (Chaves et al., 2017). Also, major colonic butyrate and propionate producers *Ruminococcaceae* and *Lachnospiraceae* (Kircher et al., 2022; Vital et al., 2017) typically inhabit the outer mucus layer (Nava et al., 2011). As *Cla1* expression is a driver of compositional changes in bank vole gut microbiota, *Cla1*-related changes in gut mucus environment may explain reduction in taxa that make the mucus layer their niche. Considering that reduction in these taxa concomitant with reduction in associated SCFAs is correlated with inflammatory bowel diseases (Venegas et al., 2019), the lack of visible inflammation is notable. Moreover, despite the reduction of *Ruminococcaceae* and *Lachnospiraceae* in contaminated areas, radionuclide exposure had no significant effect on levels of faecal butyrate or propionate. It is possible that other taxa such as *Muribaculaceae* fulfilled this service given their versatility in metabolizing complex carbohydrates (Lagkouvardos et al., 2019), providing functional redundancy.

Understanding the driver and/or function of an increase in proportion of Bacteroidetes (*Muribaculaceae*) in bank voles inhabiting contaminated areas is difficult as these bacteria form four clades that metabolise plant, host-derived and alpha glycans (two clades) (Lagkouvardos et al., 2019). Bacteroides taxa in bank voles exhibit shallow genomic divergence (Lavrinienko et al., 2020) and in this study it is not possible to determine which SVs can metabolise plant glycans, for example, and thus persist in apparent loss of host glycans (mucus) that impact *Ruminococcaceae* and *Lachnospiraceae*. With this in mind it was unfortunate that we lacked data on the amount of faecal formate. *Muribaculaceae* appears to have functions relating to formate metabolism (Lagkouvardos et al., 2019) and thus may contribute to high levels of plasma formate in bank voles inhabiting contaminated areas. Ultimately, as the ASV data is compositional in nature, it cannot be concluded whether a change in the absolute number of bacteria has affected SCFA levels.

The only faecal SCFAs responding to radionuclides were caproate and valerate, both of which are severely understudied compared with the predominant SCFAs of acetate, propionate and butyrate. While an altered gut microbiota composition may explain some impact on SCFA concentration in the faeces, the host requirements for caproate and valerate apparently are little impacted as there is no observable difference in serum concentrations associated with exposure to radionuclides. Regardless, as there is emerging evidence of serum valerate and caproate concentrations correlating with kidney and cardiovascular diseases in humans (Jadoon et al., 2018; Saresella et al., 2020), it may be relevant to include valerate and caproate among SCFAs to quantify in ecotoxicological studies if a pollutant is expected to impact kidney function.

#### 4.4. Changes in systemic availability of SCFAs associate with received dose

While luminal SCFA concentrations are net result of rates of colonic production and absorption, systemically available SCFA concentrations in plasma are additionally subject to host metabolic conditions (Boets

et al., 2017; Sakata, 2019). More than 95 % of colon-derived SCFAs are absorbed. Up to 90 % of absorbed butyrate is used by colonocytes as nutrition, whereas a large portion of absorbed propionate is utilized as a gluconeogenic substrate in the liver (Boets et al., 2017), with the rest being released into peripheral circulation. Radionuclide-related reduction in systemic availability of propionate and butyrate without corresponding changes in faecal SCFA concentrations thus could be explained by host-related processes. In humans, circulating, but not faecal, propionate and butyrate associate with metabolic parameters such as plasma glucose, and lipid metabolites, improving insulin sensitivity (Müller et al., 2019). Butyrate and propionate increase energy expenditure by upregulating the expression of transcription factor PGC-1 $\alpha$  (Gao et al., 2009; Zhan et al., 2020), which in turn stimulates fatty acid oxidation and mitochondrial biogenesis (Cheng et al., 2018). It is therefore paradoxical that here we observe reduction in circulating butyrate and propionate levels, despite our earlier findings on upregulation in transcription of PGC-1 $\alpha$  (Kesäniemi et al., 2020) and several fatty acid oxidation genes under transcriptional control of the PPAR $\alpha$ -PGC-1 $\alpha$  signaling axis (Kesäniemi et al., 2019a). More detailed experiments are required to map the flow of SCFAs both in colon and in circulation. The SCFA-metabolism mismatch is possibly a result of confounding factors, for instance due to radiation effects on mitochondrial health having its own impact on metabolism.

#### 4.5. Formate implicates issues in mitochondrial health

The significant positive correlation between circulating formate and absorbed dose rate implies an association between radionuclide exposure and one-carbon metabolism. While it is possible that an increase in circulating formate is derived from the increase in *Muribaculaceae*, most (~50 %) formate is produced (by catabolism of serine) in the mitochondria (Brosnan and Brosnan, 2016; Meiser et al., 2016). Aberrant levels of formate can be a sign of energy stress or mitochondrial dysfunction (Meiser et al., 2016). It is therefore relevant that bank voles inhabiting contaminated areas of the CEZ upregulate genes associated with fatty acid oxidation, mitochondrial biogenesis and mitochondrial oxidative stress such as *Cpt1a*, *Atf5* and *Fgf21* (Kesäniemi et al., 2020, 2019a). *Fgf21* is a pleiotropic hormone normally involved in control of energy expenditure, and although the mechanisms of *Fgf21* in mitochondrial disease vary between species (Forsström et al., 2019), its increase in serum can be an accurate biomarker for mitochondrial disease in humans and mice (Lehtonen et al., 2016). The consequences of an excess of circulating formate (formate overflow) in individual exposed to radionuclides are unknown, but for instance, catabolism of serine into formate also produces NADH and NADPH that could help maintain cellular redox balance (Fan et al., 2014). Alternatively, formate overflow is associated with poor health, such as a deficiency of folate and vitamin B-12, birth defects, and oxidative cancer (Meiser et al., 2018; Pietzke et al., 2019). Also, astronauts and *Mus musculus* experience a systemic change in mitochondrial function, particularly in mtDNA OXPHOS gene expression and integrated stress response gene expression as an apparent consequence of low dose radiation exposure during spaceflight (da Silveira et al., 2020), suggesting that mitochondrial function lies at a key position regarding metabolic responses to chronic radiation exposure. These results warrant further studies using untargeted metabolomics and a reciprocal transplant experiment to discriminate between genetic and plastic effects.

Nonetheless, an apparent lack of radionuclide impacts in faecal SCFAs with concomitant change in circulating SCFAs and our earlier data on metabolism and mitochondrial health suggests that the scenario where radionuclide exposure directly impacts the host with little effect on gut microbiota-delivered services is more likely. While here we focused on the metabolic aspects of SCFAs, there are other ways in which a shift in gut microbiota may impact host that we could not examine in this study, perhaps most interestingly the gut-brain axis. Early life gut microbiota both in the host and in the mother affect brain

development (Muhammad et al., 2022), which may explain reduction in brain mass observed in bank voles and some species of bird exposed to radionuclides (Kivisaari et al., 2020; Møller et al., 2011). Large inter-annual datasets are however required to examine developmental consequences of radionuclide exposure.

#### 4.6. Conclusions

In conclusion, we conducted a comprehensive survey of gut microbiota and aspects of host health driving gut health in a wild animal population exposed to radionuclide contamination. Exposure to radionuclides impacts gut health, physiology, and gut microbiota of bank voles. Significant changes in gut microbiota composition associated with environmental radionuclides were not accompanied by marked changes in faecal SCFA concentrations. Although we cannot test other services, such as microbiome-immunity associations, we could not find a convincing link between compositional changes and provision of services, at least for SCFAs. Radionuclide exposure likely impacts host metabolism and health directly rather than through microbially produced SCFA affecting host physiology. In turn, changes in host physiology likely affect the gut environment (mucus) that affect microbiota composition. Formate overflow provides further evidence implicating mitochondrial dysfunction as a result of chronic radiation exposure. As such, we suggest that the signatures of pollution on gut microbiota are driven by the impact on the host that in turn affects the gut microbiota, analogous to changes in stress physiology.

#### Ethics statement and benefit-sharing

Authors declare no competing interests. All experiments complied with the legal requirements and adhered closely to international guidelines for the use of animals in research. All necessary permissions were obtained from the Animal Experimentation Committee for these experiments (permission no. ESAVI/7256/04.10.07/2014). Benefits generated: Genetic resources and other data generated benefit the wider scientific community in the study of ecotoxicology in the form of a case study with a wide dataset. The research addresses questions of radionuclide contamination at a time of steeper language on part of authoritarian governments. This study was a result of international collaboration, and all major contributors and field staff working in contaminated areas are attributed as either co-authors or in acknowledgements.

#### CRedit authorship contribution statement

**Toni Jernfors:** Conceptualization, Methodology, Formal analysis, Investigation, Writing – original draft, Writing – review & editing. **Anton Lavrinienko:** Conceptualization, Methodology, Investigation, Writing – review & editing. **Igor Vareniuk:** Methodology, Investigation, Writing – review & editing. **Rikard Landberg:** Methodology, Investigation, Writing – review & editing. **Rikard Fristedt:** Methodology, Investigation, Writing – review & editing. **Olena Tkachenko:** Investigation. **Sara Taskinen:** Methodology, Formal analysis, Writing – review & editing. **Eugene Tukalenko:** Methodology, Investigation, Writing – review & editing. **Tapio Mappes:** Project administration, Supervision, Funding acquisition, Resources. **Phillip C. Watts:** Conceptualization, Supervision, Project administration, Funding acquisition, Writing – review & editing.

#### Declaration of competing interest

The authors declare that they have no known competing financial interests or personal relationships that could have appeared to influence the work reported in this paper.

#### Data availability

Sequence data are available at the European Nucleotide Archive under project accession PRJEB46797, and sample metadata, gene expression tables and SV abundance tables are available at DRYAD repository (<https://doi.org/10.5061/dryad.stjq2c79>).

#### Acknowledgements

This work was supported by funding from the Research Council of Finland (287153 and 324602 to PCW), the Finnish Cultural Foundation (to TJ) and Koneen Säätiö (to ST). We thank CSC-IT Finland ([www.csc.fi](http://www.csc.fi)) for access to computing services. We are grateful to Igor Chizhevsky, Serhii Kirieiev, and Maksym Ivanenko for logistic support and help in organising fieldwork.

#### Appendix A. Supplementary data

Supplementary data to this article can be found online at <https://doi.org/10.1016/j.scitotenv.2023.169804>.

#### References

- Acevedo-Whitehouse, K., Duffus, A.L.J., 2009. Effects of environmental change on wildlife health. *Philos. Trans. R. Soc. B* 364, 3429–3438. <https://doi.org/10.1098/rstb.2009.0128>.
- Amato, K.R., Yeoman, C.J., Kent, A., Righini, N., Carbonero, F., Estrada, A., Rex Gaskins, H., Stumpf, R.M., Yildirim, S., Torralba, M., Gillis, M., Wilson, B.A., Nelson, K.E., White, B.A., Leigh, S.R., 2013. Habitat degradation impacts black howler monkey (*Alouatta pigra*) gastrointestinal microbiomes. *ISME J.* <https://doi.org/10.1038/ismej.2013.16>.
- Anderson, M.J., 2017. Permutational Multivariate Analysis of Variance (PERMANOVA). In: Wiley StatsRef: Statistics Reference Online. John Wiley & Sons, Ltd, pp. 1–15. <https://doi.org/10.1002/9781118445112.stat07841>.
- Antwis, R.E., Beresford, N.A., Jackson, J.A., Fawkes, R., Barnett, C.L., Potter, E., Walker, L., Gaschak, S., Wood, M.D., 2021. Impacts of radiation exposure on the bacterial and fungal microbiome of small mammals in the Chernobyl Exclusion Zone. *J. Anim. Ecol.* 90, 2172–2187. <https://doi.org/10.1111/1365-2656.13507>.
- Baker, R.J., Hamilton, M.J., Van Den Bussche, R.A., Wiggins, L.E., Sugg, D.W., Smith, M.H., Lomakin, M.D., Gaschak, S.P., Bundova, E.G., Rudenskaya, G.A., Chesser, R.K., 1996. Small mammals from the most radioactive sites near the chornobyl nuclear power plant. *J. Mammal.* 77, 155–170. <https://doi.org/10.2307/1382717>.
- Baker, R.J., Dickens, B., Wickliffe, J.K., Khan, F.A.A.A., Gaschak, S., Makova, K.D., Phillips, C.D., 2017. Elevated mitochondrial genome variation after 50 generations of radiation exposure in a wild rodent. *Evol. Appl.* 10, 784–791. <https://doi.org/10.1111/eva.12475>.
- Beresford, N.A., Barnett, C.L., Gaschak, S., Maksimenko, A., Guliaichenko, E., Wood, M.D., Izquierdo, M., 2020. Radionuclide transfer to wildlife at a 'reference site' in the Chernobyl Exclusion Zone and resultant radiation exposures. *J. Environ. Radioact.* 211, 105661. <https://doi.org/10.1016/j.jenvrad.2018.02.007>.
- Birchough, G.M.H., Johansson, M.E.V., Gustafsson, J.K., Bergström, J.H., Hansson, G.C., 2015. New developments in goblet cell mucus secretion and function. *Mucosal Immunol.* 8, 712–719. <https://doi.org/10.1038/mi.2015.32>.
- Boets, E., Gomand, S.V., Deroover, L., Preston, T., Vermeulen, K., De Preter, V., Hamer, H.M., Van den Mooter, G., De Vuyst, L., Courtin, C.M., Annaert, P., Delcour, J.A., Verbeke, K.A., 2017. Systemic availability and metabolism of colonic-derived short-chain fatty acids in healthy subjects: a stable isotope study. *J. Physiol.* 595, 541–555. <https://doi.org/10.1113/JP272613>.
- Bokulich, N.A., Kaehler, B.D., Rideout, J.R., Dillon, M., Bolyen, E., Knight, R., Huttley, G.A., Gregory Caporaso, J., 2018. Optimizing taxonomic classification of marker-gene amplicon sequences with QIIME 2's q2-feature-classifier plugin. *Microbiome* 6, 90. <https://doi.org/10.1186/s40168-018-0470-z>.
- Bolyen, E., Rideout, J.R., Dillon, M.R., Bokulich, N.A., Abnet, C.C., Al-Ghalith, G.A., Alexander, H., Alm, E.J., Arumugam, M., Asnicar, F., Bai, Y., Bisanz, J.E., Bittinger, K., Brejnrod, A., Brislawn, C.J., Brown, C.T., Callahan, B.J., Caraballo-Rodríguez, A.M., Chase, J., Cope, E.K., Da Silva, R., Diener, C., Dorrestein, P.C., Douglas, G.M., Durall, D.M., Duvallet, C., Edwardson, C.F., Ernst, M., Estaki, M., Fouquier, J., Gauglitz, J.M., Gibbons, S.M., Gibson, D.L., Gonzalez, A., Gorlick, K., Guo, J., Hillmann, B., Holmes, S., Holste, H., Huttenhower, C., Huttley, G.A., Janssen, S., Jarmusch, A.K., Jiang, L., Kaehler, B.D., Kang, K.B., Keefe, C.R., Keim, P., Kelley, S.T., Knights, D., Koester, I., Kosciorek, T., Kreps, J., Langille, M.G.I., Lee, J., Ley, R., Liu, Y.-X., Loftfield, E., Lozupone, C., Maher, M., Marotz, C., Martin, B.D., McDonald, D., McIver, L.J., Melnik, A.V., Metcalf, J.L., Morgan, S.C., Morton, J.T., Naimey, A.T., Navas-Molina, J.A., Nothias, L.F., Orchanian, S.B., Pearson, T., Peoples, S.L., Petras, D., Preuss, M.L., Priesse, E., Rasmussen, L.B., Rivers, A., Robeson, M.S., Rosenthal, P., Segata, N., Shaffer, M., Shiffer, A., Sinha, R., Song, S.J., Spear, J.R., Swafford, A.D., Thompson, L.R., Torres, P.J., Trinh, P., Tripathi, A., Turnbaugh, P.J., Ul-Hasan, S., van der Hooft, J.J.J., Vargas, F., Vázquez-Baeza, Y., Vogtmann, E., von Hippel, M., Walters, W., Wan, Y., Wang, M., Warren, J., Weber, K.



- C., Williamson, C.H.D., Willis, A.D., Xu, Z.Z., Zaneveld, J.R., Zhang, Y., Zhu, Q., Knight, R., Caporaso, J.G., 2019. Reproducible, interactive, scalable and extensible microbiome data science using QIIME 2. *Nat. Biotechnol.* 37, 852–857. <https://doi.org/10.1038/s41587-019-0209-9>.
- Brila, I., Lavrinienko, A., Tukalenko, E., Ecker, F., Rodushkin, I., Kallio, E.R., Mappes, T., Watts, P.C., 2021. Low-level environmental metal pollution is associated with altered gut microbiota of a wild rodent, the bank vole (*Myodes glareolus*). *Sci. Total Environ.* 790, 148224. <https://doi.org/10.1016/j.scitotenv.2021.148224>.
- Brila, I., Lavrinienko, A., Tukalenko, E., Kallio, E.R., Mappes, T., Watts, P.C., 2023. Idiosyncratic effects of coinfection on the association between systemic pathogens and the gut microbiota of a wild rodent, the bank vole *Myodes glareolus*. *J. Anim. Ecol.* 92, 826–837. <https://doi.org/10.1111/1365-2656.13869>.
- Brosnan, M.E., Brosnan, J.T., 2016. Formate: the neglected member of one-carbon metabolism. *Annu. Rev. Nutr.* 36, 369–388. <https://doi.org/10.1146/annurev-nutr-071715-050738>.
- Bryant, D.M., Johnson, K., DiTommaso, T., Tickle, T., Couger, M.B., Payzin-Dogru, D., Lee, T.J., Leigh, N.D., Kuo, T.H., Davis, F.G., Bateman, J., Bryant, S., Guzikowski, A. R., Tsai, S.L., Coyne, S., Ye, W.W., Freeman, R.M., Peshkin, L., Tabin, C.J., Regev, A., Haas, B.J., Whited, J.L., 2017. A tissue-mapped axolotl de novo transcriptome enables identification of limb regeneration factors. *Cell Rep.* 18, 762–776. <https://doi.org/10.1016/j.celrep.2016.12.063>.
- Callahan, B.J., McMurdie, P.J., Rosen, M.J., Han, A.W., Johnson, A.J.A., Holmes, S.P., 2016. DADA2: high-resolution sample inference from Illumina amplicon data. *Nat. Methods* 13, 581–583. <https://doi.org/10.1038/nmeth.3869>.
- Caporaso, J.G., Lauber, C.L., Walters, W.A., Berg-Lyons, D., Lozupone, C.A., Turnbaugh, P.J., Fierer, N., Knight, R., 2011. Global patterns of 16S rRNA diversity at a depth of millions of sequences per sample. *Proc. Natl. Acad. Sci.* 108, 4516–4522. <https://doi.org/10.1073/pnas.100080107>.
- Car, C., Gilles, A., Armand, O., Burraco, P., Beaugelin-Seiller, K., Gashchak, S., Camilleri, V., Cavalié, I., Laloi, P., Adam-Guillermin, C., Orizaola, G., Bonzom, J.-M., 2022. Unusual evolution of tree frog populations in the Chernobyl exclusion zone. *Evol. Appl.* 15, 203–219. <https://doi.org/10.1111/eva.13282>.
- Chassaing, B., Raja, S.M., Lewis, J.D., Srinivasan, S., Gewirtz, A.T., 2017. Colonic microbiota encroachment correlates with dysglycemia in humans. *CMGH* 4, 205–221. <https://doi.org/10.1016/j.cmg.2017.04.001>.
- Chaves, B.D., Brashears, M.M., Nightingale, K.K., 2017. Applications and safety considerations of *Lactobacillus salivarius* as a probiotic in animal and human health. *J. Appl. Microbiol.* 123, 18–28. <https://doi.org/10.1111/jam.13438>.
- Chen, Yuxin, Chen, Yongsheng, Shi, C., Huang, Z., Zhang, Y., Li, S., Li, Y., Ye, J., Yu, C., Li, Z., Zhang, X., Wang, J., Yang, H., Fang, L., Chen, Q., 2018. SOAPnuke: a MapReduce acceleration-supported software for integrated quality control and preprocessing of high-throughput sequencing data. *GigaScience* 7, gix120. <https://doi.org/10.1093/gigascience/gix120>.
- Cheng, C.-F., Ku, H.-C., Lin, H., 2018. PGC-1 $\alpha$  as a pivotal factor in lipid and metabolic regulation. *Int. J. Mol. Sci.* 19, 3447. <https://doi.org/10.3390/ijms19113447>.
- Cheng, K., Brunius, C., Fristedt, R., Landberg, R., 2020. An LC-QToF MS based method for untargeted metabolomics of human fecal samples. *Metabolomics* 16, 46. <https://doi.org/10.1007/s11306-020-01669-z>.
- Chesser, R.K., Sugg, D.W., Lomakin, M.D., van den Bussche, R.A., DeWoody, J.A., Jagoe, C.H., Dallas, C.E., Whicker, F.W., Smith, M.H., Gaschak, S.P., Chizhevsky, I. V., Lyabik, V.V., Buntova, E.G., Holloman, K., Baker, R.J., 2000. Concentrations and dose rate estimates of 134137 cesium and 90 strontium in small mammals at chornobyl, Ukraine. *Environ. Toxicol. Chem.* 19, 305–312. <https://doi.org/10.1002/etc.5620190209>.
- Cortés, A., Clare, S., Costain, A., Almeida, A., McCarthy, C., Harcourt, K., Brandt, C., Tolley, C., Rooney, J., Berriman, M., Lawley, T., MacDonald, A.S., Rinaldi, G., Cantacessi, C., 2020. Baseline gut microbiota composition is associated with schistosoma mansoni infection burden in rodent models. *Front. Immunol.* 11, 1. <https://doi.org/10.3389/fimmu.2020.593838>.
- da Silveira, W.A., Fazelinia, H., Rosenthal, S.B., Laiakis, E.C., Kim, M.S., Meydan, C., Kidane, Y., Rathi, K.S., Smith, S.M., Stear, B., Ying, Y., Zhang, Y., Foox, J., Zanello, S., Crucian, B., Wang, D., Nugent, A., Costa, H.A., Zwart, S.R., Schrepfer, S., Elworth, R.A.L., Sapoval, N., Treangen, T., MacKay, M., Gokhale, N.S., Horner, S.M., Singh, L.N., Wallace, D.C., Willey, J.S., Schisler, J.C., Meller, R., McDonald, J.T., Fisch, K.M., Hardiman, G., Taylor, D., Mason, C.E., Costes, S.V., Beheshti, A., 2020. Comprehensive multi-omics analysis reveals mitochondrial stress as a central biological hub for spaceflight impact. *Cell* 183, 1185–1201.e20. <https://doi.org/10.1016/j.cell.2020.11.002>.
- Deryabina, T.G., Kuchmel, S.V., Nagorskaya, L.L., Hinton, T.G., Beasley, J.C., Lerebours, A., Smith, J.T., 2015. Long-term census data reveal abundant wildlife populations at Chernobyl. *Curr. Biol.* 25, R824–R826. <https://doi.org/10.1016/j.cub.2015.08.017>.
- Desouky, O., Ding, N., Zhou, G., 2015. Targeted and non-targeted effects of ionizing radiation. *J. Radiat. Res. Appl. Sci.* 8, 247–254. <https://doi.org/10.1016/j.jrras.2015.03.003>.
- Di Maggio, F., Minafra, L., Forte, G., Cammarata, F., Lio, D., Messa, C., Gilardi, M., Bravatà, V., 2015. Portrait of inflammatory response to ionizing radiation treatment. *J. Inflamm.* 12, 14. <https://doi.org/10.1186/s12950-015-0058-3>.
- Einor, D., Bonisoli-Alquati, A., Costantini, D., Mousseau, T.A., Möller, A.P., 2016. Ionizing radiation, antioxidant response and oxidative damage: a meta-analysis. *Sci. Total Environ.* 548–549, 463–471. <https://doi.org/10.1016/j.scitotenv.2016.01.027>.
- Fan, J., Ye, J., Kamphorst, J.J., Shlomi, T., Thompson, C.B., Rabinowitz, J.D., 2014. Quantitative flux analysis reveals folate-dependent NADPH production. *Nature* 510, 298–302. <https://doi.org/10.1038/nature13236>.
- Fernandes, A.D., Reid, J.N., Macklaim, J.M., McMurrough, T.A., Edgell, D.R., Gloor, G.B., 2014. Unifying the analysis of high-throughput sequencing datasets: characterizing RNA-seq, 16S rRNA gene sequencing and selective growth experiments by compositional data analysis. *Microbiome* 2 (12), 1–13. <https://doi.org/10.1186/2049-2618-2-15>.
- Forsström, S., Jackson, C.B., Carroll, C.J., Kuronen, M., Pirinen, E., Pradhan, S., Marmyleva, A., Auranen, M., Kleine, I.M., Khan, N.A., Roivainen, A., Marjamäki, P., Liljenbäck, H., Wang, L., Battersby, B.J., Richter, U., Velagapudi, V., Nikkanen, J., Euro, L., Suomalainen, A., 2019. Fibroblast growth factor 21 drives dynamics of local and systemic stress responses in mitochondrial myopathy with mtDNA deletions. *Cell Metab.* 30, 1040–1054.e7. <https://doi.org/10.1016/j.cmet.2019.08.019>.
- François, A., Milliat, F., Guipaud, O., Benderitter, M., 2013. Inflammation and immunity in radiation damage to the gut mucosa. *Biomed. Res. Int.* 2013. <https://doi.org/10.1155/2013/123241>.
- Frey, B., Hehlhans, S., Rödel, F., Gaip, U.S., 2015. Modulation of inflammation by low and high doses of ionizing radiation: implications for benign and malign diseases. *Cancer Lett.* 368, 230–237. <https://doi.org/10.1016/j.canlet.2015.04.010>.
- Fu, L., Niu, B., Zhu, S., Wu, S., Li, W., 2012. CD-HIT: accelerated for clustering the next-generation sequencing data. *Bioinformatics* 28, 3150–3152. <https://doi.org/10.1093/bioinformatics/bts565>.
- Gao, Z., Yin, J., Zhang, J., Ward, R.E., Martin, R.J., Lefevre, M., Cefalu, W.T., Ye, J., 2009. Butyrate improves insulin sensitivity and increases energy expenditure in mice. *Diabetes* 58, 1509–1517. <https://doi.org/10.2337/db08-1637>.
- Garnier-Laplace, J., Beaugelin-Seiller, K., Della-Vedova, C., Métivier, J.M., Ritz, C., Mousseau, T.A., Pape Möller, A., 2015. Radiological dose reconstruction for birds reconciles outcomes of Fukushima with knowledge of dose-effect relationships. *Sci. Rep.* 5, 1–13. <https://doi.org/10.1038/srep16594>.
- Gentile, C.L., Weir, T.L., 2018. The gut microbiota at the intersection of diet and human health. *Science* 362, 776–780. <https://doi.org/10.1126/science.aau5812>.
- Grabherr, M.G., Haas, B.J., Yassour, M., Levin, J.Z., Thompson, D.A., Amit, I., Adiconis, X., Fan, L., Raychowdhury, R., Zeng, Q., Chen, Z., Musceli, E., Hacohen, N., Gnirke, A., Rhind, N., di Palma, F., Birren, B.W., Nusbaum, C., Lindblad-Toh, K., Friedman, N., Regev, A., 2011. Full-length transcriptome assembly from RNA-Seq data without a reference genome. *Nat. Biotechnol.* 29, 644–652. <https://doi.org/10.1038/nbt.1883>.
- Haas, B.J., Papanicolaou, A., Yassour, M., Grabherr, M., Blood, P.D., Bowden, J., Couger, M.B., Eccles, D., Li, B., Lieber, M., MacManes, M.D., Ott, M., Orvis, J., Pochet, N., Strozzi, F., Weeks, N., Westerman, R., William, T., Dewey, C.N., Henschel, R., LeDuc, R.D., Friedman, N., Regev, A., 2013. De novo transcript sequence reconstruction from RNA-seq using the Trinity platform for reference generation and analysis. *Nat. Protoc.* 8, 1494–1512. <https://doi.org/10.1038/nprot.2013.084>.
- Han, J., Lin, K., Sequeira, C., Borchers, C.H., 2015. An isotope-labeled chemical derivatization method for the quantitation of short-chain fatty acids in human feces by liquid chromatography–tandem mass spectrometry. *Anal. Chim. Acta* 854, 86–94. <https://doi.org/10.1016/j.aca.2014.11.015>.
- Hauffe, H.C., Barelli, C., 2019. Conserve the germs: the gut microbiota and adaptive potential. *Conserv. Genet.* 20 (120), 19–27. <https://doi.org/10.1007/S10592-019-01150-Y>.
- He, J., Zhang, P., Shen, L., Niu, L., Tan, Y., Chen, L., Zhao, Y., Bai, L., Hao, X., Li, X., Zhang, S., Zhu, L., 2020. Short-chain fatty acids and their association with signalling pathways in inflammation, glucose and lipid metabolism. *Int. J. Mol. Sci.* 21, 6356. <https://doi.org/10.3390/ijms21176356>.
- Hooper, L.V., Xu, J., Falk, P.G., Midtved, T., Gordon, J.I., 1999. A molecular sensor that allows a gut commensal to control its nutrient foundation in a competitive ecosystem. *Proc. Natl. Acad. Sci.* 96, 9833–9838. <https://doi.org/10.1073/pnas.96.17.9833>.
- Hooper, L.V., Littman, D.R., Macpherson, A.J., 2012. Interactions between the microbiota and the immune system. *Science*. <https://doi.org/10.1126/science.1223490>.
- Huang, W., Guo, H.-L., Deng, X., Zhu, T.-T., Xiong, J.-F., Xu, Y.-H., Xu, Y., 2017. Short-chain fatty acids inhibit oxidative stress and inflammation in mesangial cells induced by high glucose and lipopolysaccharide. *Exp. Clin. Endocrinol. Diabetes* 125, 98–105. <https://doi.org/10.1055/s-0042-121493>.
- Iacob, S., Iacob, D.G., Luminos, L.M., 2019. Intestinal microbiota as a host defense mechanism to infectious threats. *Front. Microbiol.* 9. <https://doi.org/10.3389/fmicb.2018.03328>.
- ICRP, 2008. Environmental protection - the concept and use of reference animals and plants. *ICRP publication 108. Ann. ICRP* 38, 4–6.
- Iversen, K.N., Dicksved, J., Zoki, C., Fristedt, R., Pelve, E.A., Langton, M., Landberg, R., 2022. The effects of high fiber rye, compared to refined wheat, on gut microbiota composition, plasma short chain fatty acids, and implications for weight loss and metabolic risk factors (the RyeWeight Study). *Nutrients* 14, 1669. <https://doi.org/10.3390/nu14081669>.
- Jadoon, A., Mathew, A.V., Byun, J., Gadegbeku, C.A., Gipson, D.S., Afshinnia, F., Pennathur, S., for the Michigan Kidney Translational Core CPROBE Investigator Group, 2018. Gut microbial product predicts cardiovascular risk in chronic kidney disease patients. *Am. J. Nephrol.* 48, 269–277. <https://doi.org/10.1159/000493862>.
- Jernfors, T., Danforth, J., Kesäniemi, J., Lavrinienko, A., Tukalenko, E., Fajkus, J., Dvořáčková, M., Mappes, T., Watts, P.C., 2021. Expansion of rDNA and pericentromere satellite repeats in the genomes of bank voles *Myodes glareolus* exposed to environmental radionuclides. *Ecol. Evol.* ece3.7684. <https://doi.org/10.1002/eece3.7684>.
- Jin, Y., Wu, S., Zeng, Z., Fu, Z., 2017. Effects of environmental pollutants on gut microbiota. *Environ. Pollut.* 222, 1–9. <https://doi.org/10.1016/j.envpol.2016.11.045>.

- Jo, U., Pommier, Y., 2022. Structural, molecular, and functional insights into Schlafen proteins. *Exp. Mol. Med.* 54, 730–738. <https://doi.org/10.1038/s12276-022-00794-0>.
- Johansson, M.E.V., Gustafsson, J.K., Holmén-Larsson, J., Jabbar, K.S., Xia, L., Xu, H., Ghishan, F.K., Carvalho, F.A., Gewirtz, A.T., Sjövall, H., Hansson, G.C., 2014. Bacteria penetrate the normally impenetrable inner colon mucus layer in both murine colitis models and patients with ulcerative colitis. *Gut* 63, 281–291. <https://doi.org/10.1136/gutjnl-2012-303207>.
- Kesäniemi, J., Jernfors, T., Lavrinienko, A., Kivisaari, K., Kiljunen, M., Mappes, T., Watts, P.C., 2019a. Exposure to environmental radionuclides is associated with altered metabolic and immunity pathways in a wild rodent. *Mol. Ecol.* 15241. <https://doi.org/10.1111/mec.15241>.
- Kesäniemi, J., Lavrinienko, A., Tukalenko, E., Boratyński, Z., Kivisaari, K., Mappes, T., Milinevsky, G., Möller, A.P., Mousseau, T.A., Watts, P.C., 2019b. Exposure to environmental radionuclides associates with tissue-specific impacts on telomerase expression and telomere length. *Sci. Rep.* 9, 850. <https://doi.org/10.1038/s41598-018-37164-8>.
- Kesäniemi, J., Lavrinienko, A., Tukalenko, E., Moutinho, A.F., Mappes, T., Möller, A.P., Mousseau, T.A., Watts, P.C., 2020. Exposure to environmental radionuclides alters mitochondrial DNA maintenance in a wild rodent. *Evol. Ecol.* 34, 163–174. <https://doi.org/10.1007/s10682-019-10028-x>.
- Kim, C.H., 2021. Control of lymphocyte functions by gut microbiota-derived short-chain fatty acids. *Cell. Mol. Immunol.* 18, 1161–1171. <https://doi.org/10.1038/s41423-020-00625-0>.
- Kircher, B., Woltemate, S., Gutzki, F., Schlüter, D., Geffers, R., Bähre, H., Vital, M., 2022. Predicting butyrate- and propionate-forming bacteria of gut microbiota from sequencing data. *Gut Microbes* 14, 2149019. <https://doi.org/10.1080/19490976.2022.2149019>.
- Kivisaari, K., Boratyński, Z., Lavrinienko, A., Kesäniemi, J., Lehmann, P., Mappes, T., 2020. The effect of chronic low-dose environmental radiation on organ mass of bank voles in the Chernobyl exclusion zone. *Int. J. Radiat. Biol.* 96, 1254–1262. <https://doi.org/10.1080/09553002.2020.1793016>.
- Labocha, M.K., Schutz, H., Hayes, J.P., 2014. Which body condition index is best? *Oikos* 123, 111–119. <https://doi.org/10.1111/j.1600-0706.2013.00755.x>.
- Lagkouvardos, I., Lesker, T.R., Hitch, T.C.A., Gálvez, E.J.C., Smit, N., Neuhaus, K., Wang, J., Baines, J.F., Abt, B., Stecher, B., Overmann, J., Strowig, T., Clavel, T., 2019. Sequence and cultivation study of Muribaculaceae reveals novel species, host preference, and functional potential of this yet undescribed family. *Microbiome* 7, 1–15. <https://doi.org/10.1186/s40168-019-0637-2>.
- Langmead, B., Trapnell, C., Pop, M., Salzberg, S.L., 2009. Ultrafast and memory-efficient alignment of short DNA sequences to the human genome. *Genome Biol.* 10, R25. <https://doi.org/10.1186/gb-2009-10-3-r25>.
- Lavrinienko, A., Mappes, T., Tukalenko, E., Mousseau, T.A., Möller, A.P., Knight, R., Morton, J.T., Thompson, L.R., Watts, P.C., 2018a. Environmental radiation alters the gut microbiome of the bank vole *Myodes glareolus*. *ISME J.* 12, 2801–2806. <https://doi.org/10.1038/s41396-018-0214-x>.
- Lavrinienko, A., Tukalenko, E., Mappes, T., Watts, P.C., 2018b. Skin and gut microbiomes of a wild mammal respond to different environmental cues. *Microbiome* 6, 209. <https://doi.org/10.1186/s40168-018-0595-0>.
- Lavrinienko, A., Tukalenko, E., Kesäniemi, J., Kivisaari, K., Masiuk, S., Boratyński, Z., Mousseau, T.A., Milinevsky, G., Mappes, T., Watts, P.C., 2020. Applying the Anna Karenina principle for wild animal gut microbiota: temporal stability of the bank vole gut microbiota in a disturbed environment. *J. Anim. Ecol.* 89, 2617–2630. <https://doi.org/10.1111/1365-2656.13342>.
- Lavrinienko, A., Hämäläinen, A., Hindström, R., Tukalenko, E., Boratyński, Z., Kivisaari, K., Mousseau, T.A., Watts, P.C., Mappes, T., 2021. Comparable response of wild rodent gut microbiome to anthropogenic habitat contamination. *Mol. Ecol.* 15945. <https://doi.org/10.1111/mec.15945>.
- Lê, S., Josse, J., Hussen, F., 2008. FactoMineR: an R package for multivariate analysis. *J. Stat. Softw.* <https://doi.org/10.18637/jss.v025.i01>.
- Lehmann, P., Boratyński, Z., Mappes, T., Mousseau, T.A., Möller, A.P., 2016. Fitness costs of increased cataract frequency and cumulative radiation dose in natural mammalian populations from Chernobyl. *Sci. Rep.* 6, 19974. <https://doi.org/10.1038/srep19974>.
- Lehtonen, J.M., Forsström, S., Bottani, E., Viscomi, C., Baris, O.R., Isoniemi, H., Höckerstedt, K., Österlund, P., Hurme, M., Jylhä, J., Leppä, S., Markkula, R., Heliö, T., Mombelli, G., Uusimaa, J., Laaksonen, R., Laaksovirta, H., Auranen, M., Zeviani, M., Smeitink, J., Wiesner, R.J., Nakada, K., Isohanni, P., Suomalainen, A., 2016. FGF21 is a biomarker for mitochondrial translation and mtDNA maintenance disorders. *Neurology* 87, 2290–2299. <https://doi.org/10.1212/WNL.0000000000003374>.
- Li, B., Dewey, C.N., 2011. RSEM: accurate transcript quantification from RNA-Seq data with or without a reference genome. *BMC Bioinforma.* 12, 323. <https://doi.org/10.1186/1471-2105-12-323>.
- Loureiro, J., Mendo, S., Pereira, R., 2016. Radioactively contaminated areas: bioindicator species and biomarkers of effect in an early warning scheme for a preliminary risk assessment. *J. Hazard. Mater.* 317, 503–542. <https://doi.org/10.1016/j.jhazmat.2016.06.020>.
- Love, M.I., Huber, W., Anders, S., 2014. Moderated estimation of fold change and dispersion for RNA-seq data with DESeq2. *Genome Biol.* 15, 550. <https://doi.org/10.1186/s13059-014-0550-8>.
- Macdonald, D.W., 2006. *The Encyclopedia of Mammals*. Oxford University Press. <https://doi.org/10.1093/acref/9780199206087.001.0001>.
- Malipatil, D.K., Patel, P., Sjöberg, F., Devarakonda, S., Kalm, M., Angenete, E., Lindskog, E.B., Grandér, R., Persson, L., Stringer, A., Wilderäng, U., Swanpalmer, J., Kuhn, H.G., Steineck, G., Bull, C., 2019. Long-term mucosal injury and repair in a murine model of pelvic radiotherapy. *Sci. Rep.* 9, 4–13. <https://doi.org/10.1038/s41598-019-50023-4>.
- Mappes, T., Boratyński, Z., Kivisaari, K., Lavrinienko, A., Milinevsky, G., Mousseau, T.A., Möller, A.P., Tukalenko, E., Watts, P.C., 2019. Ecological mechanisms can modify radiation effects in a key forest mammal of Chernobyl. *Ecosphere* 10, e02667. <https://doi.org/10.1002/ecs2.2667>.
- Maurice, C.F., CL Knowles, S., Ladau, J., Pollard, K.S., Fenton, A., Pedersen, A.B., Turnbaugh, P.J., 2015. Marked seasonal variation in the wild mouse gut microbiota. *ISME J.* 9, 2423–2434. <https://doi.org/10.1038/ismej.2015.53>.
- Meiser, J., Tumanov, S., Maddocks, O., Labuschagne, C.F., Athineos, D., Van Den Broek, N., Mackay, G.M., Gottlieb, E., Blyth, K., Vousden, K., Kamphorst, J.J., Vazquez, A., 2016. Serine one-carbon catabolism with formate overflow. *Sci. Adv.* 2, 1–11. <https://doi.org/10.1126/sciadv.1601273>.
- Meiser, J., Schuster, A., Pietzke, M., Vande Voorde, J., Athineos, D., Oizel, K., Burgos-Barragan, G., Wit, N., Dhayade, S., Morton, J.P., Dornier, E., Sumpton, D., Mackay, G.M., Blyth, K., Patel, K.J., Niclou, S.P., Vazquez, A., 2018. Increased formate overflow is a hallmark of oxidative cancer. *Nat. Commun.* 9, 1368. <https://doi.org/10.1038/s41467-018-03777-w>.
- Möller, A.P., Mousseau, T.A., 2015. Strong effects of ionizing radiation from Chernobyl on mutation rates. *Sci. Rep.* 5, 8363. <https://doi.org/10.1038/srep08363>.
- Möller, A.P., Mousseau, T.A., 2018. Reduced colonization by soil invertebrates to irradiated decomposing wood in Chernobyl. *Sci. Total Environ.* 645, 773–779. <https://doi.org/10.1016/j.scitotenv.2018.07.195>.
- Möller, A.P., Bonisoli-Alquati, A., Rudolfsen, G., Mousseau, T.A., 2011. Chernobyl birds have smaller brains. *PLoS One* 6, e16862. <https://doi.org/10.1371/journal.pone.0016862>.
- Möller, A.P., Bonisoli-Alquati, A., Mousseau, T.A., 2013. High frequency of albinism and tumours in free-living birds around Chernobyl. *Mutat. Res./Genet. Toxicol. Environ. Mutagen.* 757, 52–59. <https://doi.org/10.1016/j.mrgentox.2013.04.019>.
- Morley, N.J., 2012. The effects of radioactive pollution on the dynamics of infectious diseases in wildlife. *J. Environ. Radioact.* 106, 81–97. <https://doi.org/10.1016/j.jenvrad.2011.12.019>.
- Moussa, L., Unsunier, B., Demarquay, C., Benderitter, M., Tamarat, R., Sémont, A., Mathieu, N., 2016. Bowel radiation injury: complexity of the pathophysiology and promises of cell and tissue engineering. *Cell Transplant.* 25, 1723–1746. <https://doi.org/10.3727/096368916X691664>.
- Mousseau, T.A., 2021. The biology of Chernobyl. *Annu. Rev. Ecol. Evol. Syst.* 52, 87–109. <https://doi.org/10.1146/annurev-ecolsys-110218-024827>.
- Moya, A., Ferrer, M., 2016. Functional redundancy-induced stability of gut microbiota subjected to disturbance. *Trends in Microbiology, Special Issue: Microbial Endurance* 24, 402–413. <https://doi.org/10.1016/j.tim.2016.02.002>.
- Muhammad, F., Fan, B., Wang, R., Ren, J., Jia, S., Wang, L., Chen, Z., Liu, X.-A., 2022. The molecular gut-brain axis in early brain development. *Int. J. Mol. Sci.* 23, 15389. <https://doi.org/10.3390/ijms232315389>.
- Müller, M., Hernández, M.A.G., Goossens, G.H., Reijnders, D., Holst, J.J., Jocken, J.W.E., van Eijk, H., Canfora, E.E., Blaak, E.E., 2019. Circulating but not faecal short-chain fatty acids are related to insulin sensitivity, lipolysis and GLP-1 concentrations in humans. *Sci. Rep.* 9 (19), 1–9. <https://doi.org/10.1038/s41598-019-48775-0>.
- Mustonen, V., Kesäniemi, J., Lavrinienko, A., Tukalenko, E., Mappes, T., Watts, P.C., Juvansuu, J., 2018. Fibroblasts from bank voles inhabiting Chernobyl have increased resistance against oxidative and DNA stresses. *BMC Cell Biol.* 19, 17. <https://doi.org/10.1186/s12860-018-0169-9>.
- Nakazawa, M., 2019. *fmsb: Functions for Medical Statistics Book With Some Demographic Data. R Package Version 0.7.0*.
- Nava, G.M., Friedrichsen, H.J., Stappenbeck, T.S., 2011. Spatial organization of intestinal microbiota in the mouse ascending colon. *ISME J.* 5, 627–638. <https://doi.org/10.1038/ismej.2010.161>.
- Nyström, E.E.L., Birchenough, G.M.H., van der Post, S., Arike, L., Gruber, A.D., Hansson, G.C., Johansson, M.E.V., 2018. Calcium-activated chloride channel regulator 1 (CLCA1) controls mucus expansion in colon by proteolytic activity. *EBioMedicine* 33, 134–143. <https://doi.org/10.1016/j.ebiom.2018.05.031>.
- Oksanen, J., Blanchet, F.G., Kindt, R., Legend, P., Minchin, P.R., Hara, R.B.O., Simpson, G.L., Soly, P., Stevens, M.H.H., Wagner, H., 2018. *Package 'vegan' Version 2.5-2. Community Ecology Package*.
- Paone, P., Cani, P.D., 2020. Mucus barrier, mucins and gut microbiota: the expected slimy partners? *Gut* 69, 2232–2243. <https://doi.org/10.1136/gutjnl-2020-322260>.
- Park, S.W., Zhen, G., Verhaeghe, C., Nakagami, Y., Nguyen, L.T., Barczak, A.J., Killeen, N., Erle, D.J., 2009. The protein disulfide isomerase AGR2 is essential for production of intestinal mucus. *Proc. Natl. Acad. Sci. U. S. A.* 106, 6950–6955. <https://doi.org/10.1073/pnas.0808722106>.
- Pickard, J.M., Zeng, M.Y., Caruso, R., Núñez, G., 2017. Gut microbiota: role in pathogen colonization, immune responses, and inflammatory disease. *Immunol. Rev.* 279, 70–89. <https://doi.org/10.1111/immr.12567>.
- Pietzke, M., Meiser, J., Vazquez, A., 2019. Formate metabolism in health and disease. *Mol. Metab.* 1–15. <https://doi.org/10.1016/j.molmet.2019.05.012>.
- Redfern, L.K., Jayasundara, N., Singleton, D.R., Di Giulio, R.T., Carlson, J., Sumner, S.J., Gunsch, C.K., 2021. The role of gut microbial community and metabolic shifts in adaptive resistance of Atlantic killifish (*Fundulus heteroclitus*) to polycyclic aromatic hydrocarbons. *Sci. Total Environ.* 776, 145955. <https://doi.org/10.1016/j.scitotenv.2021.145955>.
- Richardson, J.B., Dancy, B.C.R., Horton, C.L., Lee, Y.S., Madejczyk, M.S., Xu, Z.Z., Ackermann, G., Humphrey, G., Palacios, G., Knight, R., Lewis, J.A., 2018. Exposure to toxic metals triggers unique responses from the rat gut microbiota. *Sci. Rep.* 8, 6578. <https://doi.org/10.1038/s41598-018-24931-w>.

- Rodgers, B.E., Baker, R.J., 2000. Frequencies of micronuclei in bank voles from zones of high radiation at Chernobyl, Ukraine. *Environ. Toxicol. Chem.* 19, 1644–1648. <https://doi.org/10.1002/etc.5620190623>.
- Rodgers, B.E., Wickliffe, J.K., Phillips, C.J., Chessier, R.K., Baker, R.J., 2001. Experimental exposure of naive bank voles (*Clethrionomys glareolus*) to the Chernobyl, Ukraine, environment: a test of radioresistance. *Environ. Toxicol. Chem.* 20, 1936–1941. <https://doi.org/10.1002/etc.5620200911>.
- Rojo, D., Gosálbes, M.J., Ferrari, R., Pérez-Cobas, A.E., Hernández, E., Oltra, R., Buesa, J., Latorre, A., Barbas, C., Ferrer, M., Moya, A., 2015. *Clostridium difficile* heterogeneously impacts intestinal community architecture but drives stable metabolome responses. *ISME J.* 9, 2206–2220. <https://doi.org/10.1038/ismej.2015.32>.
- Rudolph, K., Schneider, D., Fichtel, C., Daniel, R., Heistermann, M., Kappeler, P.M., 2022. Drivers of gut microbiome variation within and between groups of a wild Malagasy primate. *Microbiome* 10, 28. <https://doi.org/10.1186/s40168-021-01223-6>.
- Sakata, T., 2019. Pitfalls in short-chain fatty acid research: a methodological review. *Anim. Sci. J.* 90, 3–13. <https://doi.org/10.1111/asj.13118>.
- Saresella, M., Marventano, I., Barone, M., La Rosa, F., Piancone, F., Mendozzi, L., d'Arma, A., Rossi, V., Pugnetti, L., Roda, G., Casagni, E., Cas, M.D., Paroni, R., Brigidi, P., Turroni, S., Clerici, M., 2020. Alterations in Circulating Fatty Acid Are Associated With Gut Microbiota Dysbiosis and Inflammation in Multiple Sclerosis. *Frontiers in Immunology* 11.
- Schneider, C.A., Rasband, W.S., Eliceiri, K.W., 2012. NIH image to ImageJ: 25 years of image analysis. *Nat. Methods* 9, 671–675. <https://doi.org/10.1038/nmeth.2089>.
- Schroeder, B.O., 2019. Fight them or feed them: how the intestinal mucus layer manages the gut microbiota. *Gastroenterol. Rep.* 7, 3–12. <https://doi.org/10.1093/gastro/goy052>.
- Segata, N., Izard, J., Waldron, L., Gevers, D., Miropolsky, L., Garrett, W.S., Huttenhower, C., 2011. Metagenomic biomarker discovery and explanation. *Genome Biol.* 12 <https://doi.org/10.1186/gb-2011-12-6-r60>.
- Shreiner, A.B., Kao, J.Y., Young, V.B., 2015. The gut microbiome in health and in disease. *Curr. Opin. Gastroenterol.* 31, 69–75. <https://doi.org/10.1097/MOG.0000000000000139>.
- Simão, F.A., Waterhouse, R.M., Ioannidis, P., Kriventseva, E.V., Zdobnov, E.M., 2015. BUSCO: assessing genome assembly and annotation completeness with single-copy orthologs. *Bioinformatics* 31, 3210–3212. <https://doi.org/10.1093/bioinformatics/btv351>.
- Suvama, K.S., Layton, C., Bancroft, J.D., 2013. *Bancroft's Theory and Practise of Histological Techniques*, 7th edition. Churchill Livingstone, London, UK.
- The R Core Team, 2018. R: A Language and Environment for Statistical Computing. R Foundation for Statistical Computing, Vienna, Austria. URL: <http://www.R-project.org/>. <https://doi.org/10.1038/sj.hdy.6800737>.
- Tian, L., Wang, X.-W., Wu, A.-K., Fan, Y., Friedman, J., Dahlin, A., Waldor, M.K., Weinstock, G.M., Weiss, S.T., Liu, Y.-Y., 2020. Deciphering functional redundancy in the human microbiome. *Nat. Commun.* 11, 6217. <https://doi.org/10.1038/s41467-020-19940-1>.
- van der Hee, B., Wells, J.M., 2021. Microbial regulation of host physiology by short-chain fatty acids. *Trends Microbiol.* 29, 700–712. <https://doi.org/10.1016/j.tim.2021.02.001>.
- Venegas, D.P., De La Fuente, M.K., Landskron, G., González, M.J., Quera, R., Dijkstra, G., Harmsen, H.J.M., Faber, K.N., Hermoso, M.A., 2019. Short chain fatty acids (SCFAs) mediated gut epithelial and immune regulation and its relevance for inflammatory bowel diseases. *Front. Immunol.* 10, 277. <https://doi.org/10.3389/FIMMU.2019.00277/BIBTEX>.
- Vital, M., Howe, A.C., Tiedje, J.M., 2014. Revealing the bacterial butyrate synthesis pathways by analyzing (meta)genomic data. *mBio* 5. <https://doi.org/10.1128/mbio.00889-14>.
- Vital, M., Karch, A., Pieper, D.H., 2017. Colonic butyrate-producing communities in humans: an overview using omics data. *mSystems* 2. <https://doi.org/10.1128/mSystems.00130-17>.
- Watts, P.C., Mappes, T., Tukalenko, E., Mousseau, T.A., Boratyński, Z., Möller, A.P., Lavrinienko, A., 2022. Interpretation of gut microbiota data in the 'eye of the beholder': a commentary and re-evaluation of data from 'Impacts of radiation exposure on the bacterial and fungal microbiome of small mammals in the Chernobyl Exclusion Zone'. *J. Anim. Ecol.* 91, 1535–1545. <https://doi.org/10.1111/1365-2656.13667>.
- Young, M.D., Wakefield, M.J., Smyth, G.K., Oshlack, A., 2010. Gene ontology analysis for RNA-seq: accounting for selection bias. *Genome Biol.* 11, R14. <https://doi.org/10.1186/gb-2010-11-2-r14>.
- Zhan, K., Yang, T.Y., Chen, Y., Jiang, M.C., Zhao, G.Q., 2020. Propionate enhances the expression of key genes involved in the gluconeogenic pathway in bovine intestinal epithelial cells. *J. Dairy Sci.* 103, 5514–5524. <https://doi.org/10.3168/jds.2019-17309>.
- Zhang, L., Nichols, R.G., Correll, J., Murray, I.A., Tanaka, N., Smith, P.B., Hubbard, T.D., Sebastian, A., Albert, I., Hatzakis, E., Gonzalez, F.J., Perdew, G.H., Patterson, A.D., 2015. Persistent organic pollutants modify gut microbiota-host metabolic homeostasis in mice through aryl hydrocarbon receptor activation. *Environ. Health Perspect.* 123, 679–688. <https://doi.org/10.1289/ehp.1409055>.